Photothermal and photovoltaic properties of transparent thin films of porphyrin compounds for energy applications 🄵

🆔 Jou Lin, and 🆔 Donglu Shi

COLLECTIONS

🄵 This paper was selected as Featured

View Online   Export Citation   CrossMark

ARTICLES YOU MAY BE INTERESTED IN

Biological function following radical photo-polymerization of biomedical polymers and surrounding tissues: Design considerations and cellular risk factors
Applied Physics Reviews **8**, 011301 (2021); https://doi.org/10.1063/5.0015093

Noise spectroscopy of molecular electronic junctions
Applied Physics Reviews **8**, 011303 (2021); https://doi.org/10.1063/5.0027602

Recent progress and prospects of integrated perovskite/organic solar cells
Applied Physics Reviews **7**, 031303 (2020); https://doi.org/10.1063/5.0013912

AIP Publishing

Photothermal and photovoltaic properties of transparent thin films of porphyrin compounds for energy applications ⓕ

View Online   Export Citation   CrossMark

Jou Lin ⓘ and Donglu Shi[a) ⓘ

AFFILIATIONS

The Materials Science and Engineering Program, Department of Mechanical and Materials Engineering, College of Engineering and Applied Science, University of Cincinnati, Cincinnati, Ohio 45221, USA

[a)]Author to whom correspondence should be addressed: donglu.shi@uc.edu

ABSTRACT

To address the critical issues in solar energy, the current research has focused on developing advanced solar harvesting materials that are low cost, lightweight, and environmentally friendly. Among many organic photovoltaics (PVs), the porphyrin compounds exhibit unique structural features that are responsible for strong ultraviolet (UV) and near infrared absorptions and high average visible transmittance, making them ideal candidates for solar-based energy applications. The porphyrin compounds have also been found to exhibit strong photothermal (PT) effects and recently applied for optical thermal insulation of building skins. These structural and optical properties of the porphyrin compounds enable them to function as a PT or a PV device upon sufficient solar harvesting. It is possible to develop a transparent porphyrin thin film with PT- and PV-dual-modality for converting sunlight to either electricity or thermal energy, which can be altered depending on energy consumption needs. A building skin can be engineered into an active device with the PT- and PV-dual modality for large-scale energy harvesting, saving, and generation. This review provides the current experimental results on the PT and PV properties of the porphyrin compounds such as chlorophyll and chlorophyllin. Their PT and PV mechanisms are discussed in correlations to their electronic structures. Also discussed are the synthesis routes, thin film deposition, and potential energy applications of the porphyrin compounds.

Published under license by AIP Publishing https://doi.org/10.1063/5.0036961

TABLE OF CONTENTS

I. INTRODUCTION

The pressing issues in energy sustainability call for novel approaches in generating inexhaustible energy without compromising

the energy sources in the future. Solar harvesting for energy sustainability has been an intense research area that focuses on various advanced material based technologies among which solar cells have been the major approach for converting photons directly to electricity by the photovoltaic (PV) effect. There are other photon energy conversion mechanisms such as the photothermal (PT) effect that has been extensively studied for biomedical therapeutics.[1–8] In biomedical diagnosis and therapeutics, the PT materials are typically made of photon-absorbing metallic conductors such as gold and graphene that exhibit strong photothermal effects capable of raising the local temperature to the hyperthermia treatment range of $\sim 45\,^\circ$C. These PT materials are often synthesized into small quantities in milligrams and dispersed in aqueous solutions for intravenous delivery. The excitation light source for photothermal treatment mainly employs near infrared (NIR) laser (typically 708 and 808 nm) for significant NIR absorption and tissue penetration. The typical PT materials include inorganic materials (i.e., noble metals),[2,3] carbon-based materials,[4,5] Fe_3O_4 and its composites,[6,7] organic materials (i.e., polymer-based nanomaterials),[8,9] and porphyrin compounds[10–14].

Only recently, the PT effect in the thin film form has been explored for energy applications with white light excitation.[6,7,15–18] The residential and commercial building sectors account for about 40% (or about 40 quadrillion British thermal units) of the total U.S. energy consumption.[19] Thermal insulation has been conventionally achieved by various glazing technologies. Single-panes are, however, practically not viable due to rapid heat loss in the winter especially in northern America. A new concept of "optical thermal insulation" (OTI) was recently proposed and realized via PT film coated single-pane windows without any intervention medium.[6,15–18] Zhao *et al.* first reported the coating of a thin film containing Fe_3O_4 nanoparticles on glass for energy-efficient window applications.[6] As shown in Fig. 1, if a spectral-selective PT thin film is applied on a window inner surface, the window surface temperature can increase from $25\,^\circ$C to $> 50\,^\circ$C upon solar irradiation. The window thermal transmittance depends on the temperature difference, ΔT, between the single-pane (without glazing) and the room interior. Due to

photothermal heating, the reduction in ΔT will effectively lower heat transfer through the building skin, characterized by a low U-factor (the U-factor is essentially the thermal transmittance) without double- or triple-glazing.

OTI requires special optical spectra of the PT films, i.e., strong ultraviolet (UV) and NIR absorptions and high visible transmittance (AVT).[19] The strong absorptions in the UV and NIR regions ensure significant solar light harvesting for conversion to heat, while high AVT provides the visible transparency of the window. These particular spectral requirements of PT are also shared by transparent PV panels. Another common feature of PV and PT panels lies on a large two-dimensional (2D) surface area for sufficient solar light harvest. According to the National Renewable Energy Laboratory, supplying all electricity needs of the U.S. with photovoltaic solar energy would require 1948 ft^2 per person.[20] To effectively utilize surface areas, large-area building skins can be engineered into PT or PV panels for solar light harvesting, specifically those modern buildings with glass façade (Fig. 2). This approach is particularly effective in the population-concentrated urban areas and megacities with high densities of buildings. In this approach, the building skin is not only a "window" enframed within the building walls that compromise between lighting and heat loss, but also a PV or PT device capable of solar harvesting, energy conversion, and production of both heat and electricity simultaneously or alternatively in dual modality modes.

The key challenges in achieving successful dual-modality include particulate materials that have to be structurally and spectrally tailored in the PT and PV thin films on building skins. As is well-known, the basic requirement is efficient solar harvesting within certain spectra, typically in the three regions: ultraviolet (UV), visible, and infrared (IR), respectively, with corresponding wavelengths of 100–400 nm, 400–700 nm, and above 700 nm. According to the solar spectra, the infrared provides solar energy around 49.4% and visible light 42.3%, while UV radiation only contributes 8.3% at ground level.[21,22] Therefore, material design and structure development need to
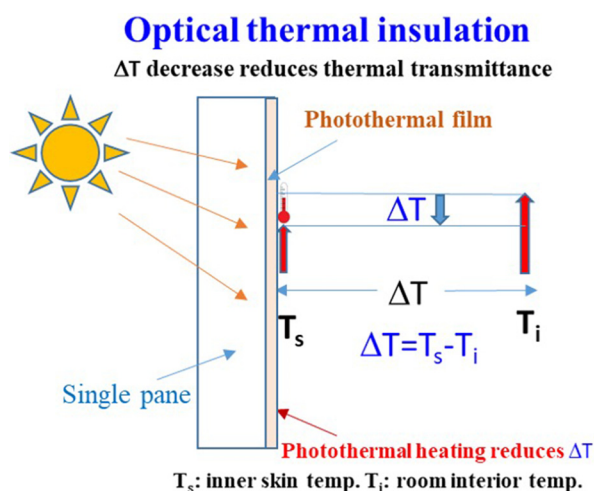

FIG. 1. Schematic working principle of photothermal film.

FIG. 2. Optical photograph of a modern building with glass facade.

consider harvesting most of the infrared radiation for efficient energy conversion and utilization.

Transparent PT and PV thin films require high visible transmittance specifically for building skins. This unique characteristic necessitates spectral selective materials (and structures) that are strongly absorbent in the UV and NIR regions but highly transparent in the visible band with a saddle-like (or U-shaped) spectrum, as schematically represented in Fig. 3(a). As can be seen in this figure, while gold nanoparticles exhibit strong absorption below 300 nm, there is another peak at 520 nm, contributing to considerable visible light absorption. Much stronger absorption is observed in the UV range for graphene and Fe_3O_4 nanoparticles, but it gradually decays to the minimum in the visible range up to near-infrared (NIR). All conducting materials with high charge densities exhibit strong photothermal effects but lacking sufficient visible transmittance. Among most of the PT materials, chlorophyll shows a saddle-like spectrum with two peaks, respectively, at 415 nm (UV) and 664 nm (NIR), which is ideal for PT–PV dual modality building skin applications since it exhibits both the PT and PV effects [Fig. 3(a)].

Chlorophyll belongs to the porphyrin compounds that are structurally characterized with a large ring molecule consisting of four pyrroles, denoted as the porphyrin ring. The tetrapyrroles are smaller rings made of four carbons and one nitrogen. The porphyrin compounds typically have a metal ion at the center of the tetrapyrrole ring.[23] By alternating the chelated ion, different porphyrin compounds can be formed. Replacing the central metal ion is normally achieved by using strong acids as the reaction media.[24] Interestingly, some porphyrins occur in nature such as chlorophyll, heme, and hemoglobin (HB). As is well-known, chlorophyll is an essential component in plants for photosynthesis. Its chemical structure is featured with a magnesium atom at the center of the tetrapyrrole ring. The saddle-like absorption [Fig. 3(a)] is particularly sought after for transparent solar harvesting devices. Similar to chlorophyll, most of the porphyrin compounds exhibit two main peaks in the absorption spectra, denoted as Soret bands (380–500 nm) and Q bands (500–750 nm).[25] These optical characteristics tend to render the porphyrins with unique colors, making them important "dyes" in the paper and textile industries.[26] The strong absorptions in these particular bands have also been utilized for

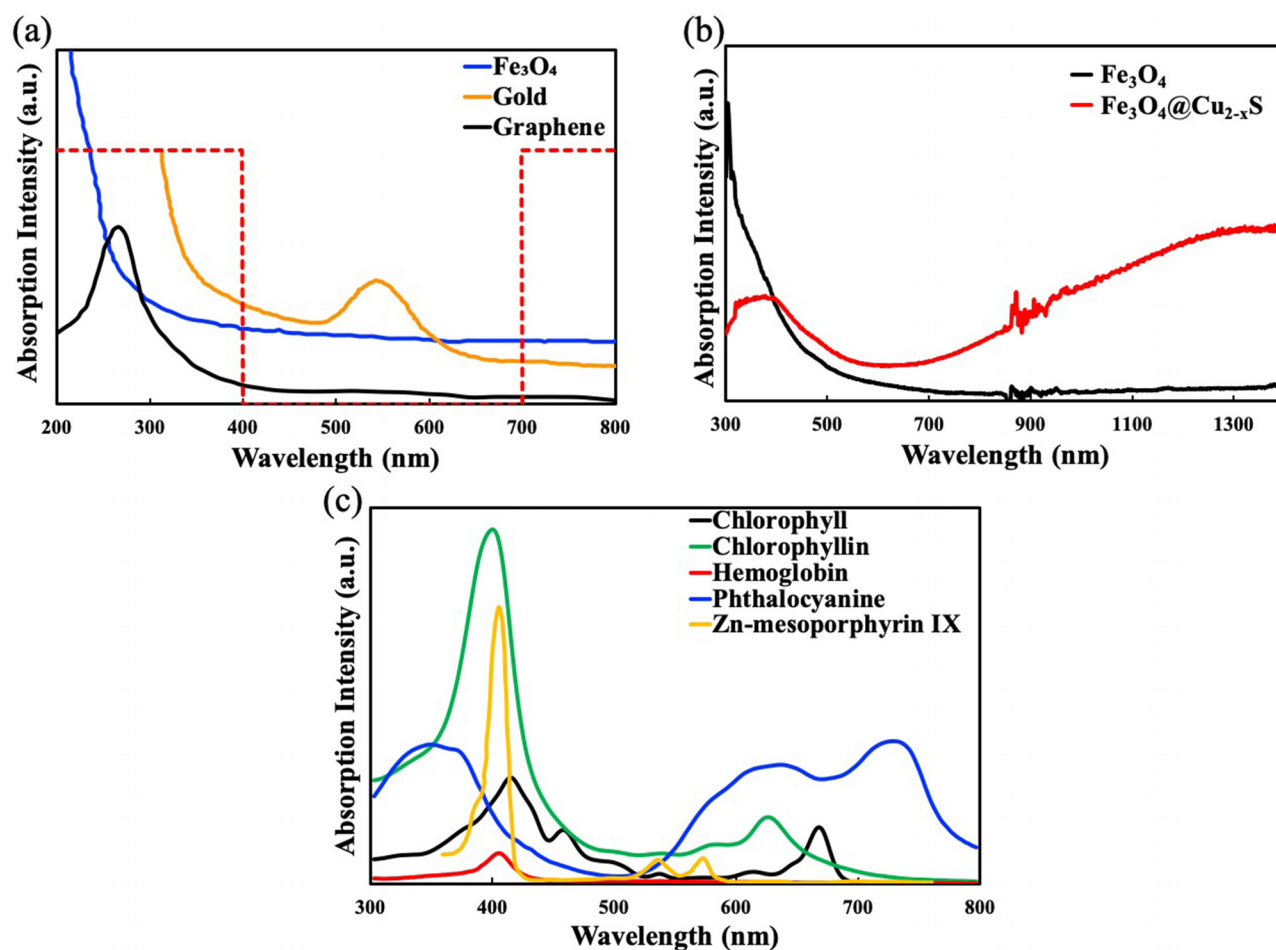**FIG. 3.** (a) Comparison of spectra of gold, graphene, and Fe_3O_4; an ideal absorption spectrum (the dashed line) is schematically shown for highly transparent thin films, (b) absorption of $Fe_3O_4@Cu_{2-x}S$ showing its broad NIR absorptions (include the spectrum of Fe_3O_4 here for comparison), and (c) absorption spectra of porphyrins: chlorophyll, chlorophyllin, hemoglobin, phthalocyanine, and zinc-mesoporphyrin IX.

photothermal applications in biomedicine, energy,[11–16,18] and photovoltaics.[27–35,37]

To enhance NIR absorption, Lin *et al.* modified Fe_3O_4 by addition of $Cu_{2-x}S$ and developed the $Fe_3O_4@Cu_{2-x}S$ thin films.[17] Comparing with the Fe_3O_4 thin films, the $Fe_3O_4@Cu_{2-x}S$ thin film is spectrally characterized with a much stronger NIR absorbance [Fig. 3(b)], contributing to an increased photothermal efficiency under simulated solar irradiation. Due to the modified structure and NIR absorption, the photothermal effect is considerably enhanced in $Fe_3O_4@Cu_{2-x}S$.[17] For transparent PV and PT thin films, more refined absorptions near UV and NIR can be obtained in the porphyrin compound as shown in Fig. 3(c). Both chlorophyll and chlorophyllin thin films have been developed with rather sharp peaks around 400 and 700 nm, giving distinctive optical characteristics of these materials for a variety of applications.[15,18] Multilayer chlorophyll films were also deposited on glass substrates showing excellent photothermal property and transparency. The photothermal mechanism of porphyrins was identified based on the photon-activated molecular resonance.[16]

This review presents the most recent experimental results on structures and properties of the porphyrin compounds for promising energy applications. The fundamental photothermal mechanisms are discussed based on their photon–molecular interactions based on the Raman spectra. The photothermal properties of the porphyrin compounds are characterized and calculated including *U*-factor, specific absorption rate (SAR), specific photothermal coefficient (SPC), and photothermal conversion efficiency. The current status of porphyrin-based solar cells is also discussed on the solar cell structure, I–V curve, and efficiency. The prospect of PT–PV dual modality film design will be introduced for future studies.

II. PORPHYRIN COMPOUNDS AND THE DERIVATIVES
A. Structural characteristics of porphyrin

The porphyrin compounds are naturally occurring and characterized with the porphyrin ring structures[36] that are typically found in chlorophyll[37] and heme of hemoglobin.[38] Due to the ring structure of the conjugated double bonds of porphyrins, porphyrin and its derivatives show unique absorption spectra, emission, charge transfer, and chelating properties. The chemical and physical mechanisms of porphyrins are responsible for electron transfer, oxygen binding, photochemical, and photosynthesis. These unique structures and properties of the porphyrin compounds have been utilized in biomedical and energy applications including photodynamic/photothermal therapy (PTT),[39–41] molecular electronic devices,[42] and solar energy conversion.[27–35]

Figure 3(c) shows the unique bands of porphyrins in the absorption spectra. As shown in this figure, the Soret and Q bands are, respectively, in the 380–500 nm (blue) and the 500–750 nm ranges. The wavelength shifts and absorbance changes of porphyrins are dependent on the solvent, pH value, temperature, central metal ions, etc.[23,43–46] UV-vis spectra reflect the key structural features that are responsible for the chemical characteristics and physical properties of the porphyrin compounds. As the absorption peaks of the porphyrin compounds are within the main emission spectrum of solar radiation, the photons can be effectively harvested and converted to other forms of energy such as heat and electricity. For applications that require certain transparency of the thin films, the absorptions are required to be isolated in the UV and NIR regions (Fig. 3). For medical applications

such as photothermal therapy, strong NIR absorption is preferred for its deeper tissue penetration.[47]

B. The chemical characteristics and synthesis of porphyrins

The molecular structure of a porphyrin consists of a union of four pyrrole rings (one nitrogen and four carbon atoms) linked by methine bridges (—CH=) to form a macrocycle (Fig. 4). Porphyrins behave as the tetradentate ligands for chelating metals with four nitrogen atoms holding the metal ions in the center. The central metal ions act as Lewis acids for accepting electron pairs from dianionic porphyrin ligands. The porphyrin structure shows two main linker positions, β-positions and meso-positions. There are eight β-positions located in the pyrrole group and four meso-positions located at the methine bridge. The natural porphyrins exhibit β-positions linked like chlorophyll and heme, based on which the meso-porphyrins can be developed as the functional artificial compounds. The porphyrin active sites depend on electronegativity, which can be controlled by selecting the metals coordinated to the central nitrogen atoms. Carrying divalent central metals can provide the electronegative porphyrin ligands to be substituted on the meso-carbon sites, resulting in stable metalloporphyrin.[48–51]

Tremendous synthetic procedures have been reported[52–58] based on the molecular structures of porphyrins. In principle, there are many chemical strategies to synthesize and modify porphyrins, including different pyrrole,[52,53,57] aldehyde,[53,54,57] dipyrromethene,[55] and tripyrrane.[56] The first study on porphyrin synthesis was carried out in 1935 by Rothemund[52] They reported porphyrin synthesis by mixing pyrrole and aldehyde, and heating them up in a sealed tube. This approach was later modified by using pyrrole and formaldehyde to form a porphyrin with meso-position substitutions.[53] Further improvements were made by involving an acid catalyzed pyrrole and aldehyde condensation to react in open air.[54] Consequently, Lindsey *et al.*[57] optimized this process by reacting pyrrole and benzaldehyde reversibly at room temperature. Lee *et al.* presented a one-flask synthesis of meso-porphyrins by using pyrrole and dipyrromethane. Boudif and Momenteau[56] proposed a so-called "3 + 1" synthetic strategy of porphyrins. In this approach, the porphyrin macrocycle was obtained by mixing acid-catalyzed condensation pyrrole with tripyrrane. Although either diformylpyrrole or tripyrrane must be symmetrical to
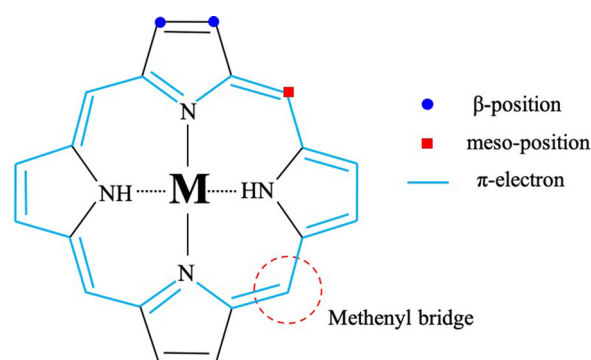

FIG. 4. Molecular structure of porphyrin (M represent metal ions, such as Mg^{2+}, Cu^{2+}, Fe^{2+}, Zn^{2+}, etc.).

remove isomers and recrystallization,[58] these porphyrins all exhibit two sub-equal intensity signals in the proton nuclear magnetic resonance (NMR) spectra.

C. Electronic structures and absorptions of porphyrins

According to Hückel's rule (the planar molecule is considered aromatic which has $4n + 2 \pi$ electrons), the porphyrin ring is a conjugated molecule containing 18π electrons. Both Soret and Q bands attributing to the $\pi-\pi^*$ transitions can be explained by the Gouterman model (so-called four-orbital model). The Soret bands (or B bands) are given by a strong transition to the second excited state and the Q bands are associated with a weak transition to the first excited state. Gouterman[25] proposed the four-orbital model to explain the porphyrins absorption spectra based on the electron transitions between highest occupied molecular orbitals (HOMOs) and lowest unoccupied molecular orbitals (LUMOs), as shown in Fig. 5. The relative transition energy is affected by the central metal ions and the substituents in the ring.

There two symmetries are denoted as b_1 (a_{2u}) and b_2 (a_{1u}) in HOMO and c_1 (e_{gx}) and c_2 (e_{gy}) in LUMO. Due to the configuration interaction of electronic transitions $a_{1u} \rightarrow e_g$ and $a_{2u} \rightarrow e_g$, the transitions between these orbitals provide two excited states. The mixing of orbital splits these two excited states in energy, resulting in two symmetrical states (^1E_u) (Fig. 6). The higher energy state with greater oscillator strength is responsible for the B-bands, while the lower energy state with weaker oscillator strength gives rise in the Q-bands.

The absorption spectra are affected by the differences in the conjugation and symmetry of a porphyrin.[25,48,59] The electronic structure of a metalloporphyrin can be changed by different central metal substituent in the porphyrin ring. Shelnutt and Ortiz[60] reported that the a_{1u} orbital energy would not be affected by metal substitution because it has nodes through the nitrogen atoms (pyrroles); therefore, it incapable of interacting with the metal orbitals. The a_{2u} orbital energy, on the other hand, is expected to be changed by metal substituents. Gouterman[25] reported that the a_{2u} orbital energies are influenced by
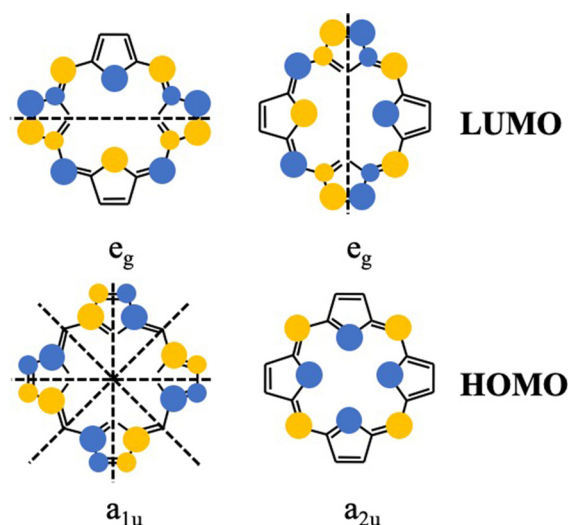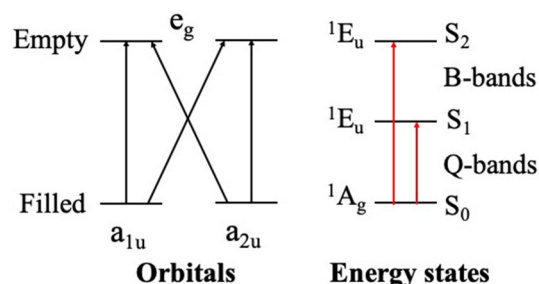

FIG. 6. Orbitals and energy states diagrams showing possible transitions for porphyrins. The actual relative energies depend on the substituents on the rings.

the p orbital of metals. The orbital energy rises with more electropositivity, resulting in red-shift (Q bands) and intensified visible band. The extent of delocalization of the electron a_{2u} orbital into the p_z orbital of metal increases with electronegativity. The a_{2u} stabilization is also ascribed to the interaction with an empty metal p_z orbital.

The electronic structure of the metalloporphyrin can be modified by changing the substitutes at the β- or meso-positions of the ring.[60,61] The a_{1u} orbital energy can be altered by changing the substituents at the β-positions since a_{1u} has more β-carbons of pyrrole rings than a_{2u}. Comparatively, the a_{2u} orbitals are strongly influenced by metal and meso substituents because the symmetry allowed interacting with the p orbital of the metal and the considerable charge on the meso carbons.[60] Shelnutt and Ortiz reported that strong conjugation of the π-electron system of the vinyl group with the ring can improve the delocalization of the ring charge exceeding the α-carbons of the vinyl. This strong conjugation of the π-electron system further lowers the configuration-interaction (CI) for protoporphyrin IX. Liao and Scheiner[61] found a strong electron effect in metalloporphyrin by replacing the meso phenyl group and β-pyrrolic hydrogen (H) with fluorine (F) atoms for its strong electron-withdrawing effect. Ram Kumar et al. synthesized A_3B type meso substituted porphyrin containing three thienyl groups and one phenyl group, and explained the orbital differences between thienyl ring and phenyl group by the density functional theory (DFT). The p-orbital delocalization can be enhanced leading to red-shift in the emission spectrum due to the co-planar of the thienyl groups/phenyl groups with the dihedral angles. They also found that the a_{2u} and e_{gx} energy levels are associated with the redox phenomenon of the porphyrins. In particular, the lower a_{2u} energy results in lower oxidation potentials for the porphyrins, and the lower e_{gx} energy indicates higher reduction potential. Furthermore, the electronic structure of a metalloporphyrin can be altered by ligand coordination to the axial positions on the metal.[61] The ligands will enhance or inhibit the ability of metal to withdraw electrons from the π-system of porphyrins, so that the electron structure is modified via these axial ligands. The axial coordination to the high molecular symmetry (square-planar, D_{4h}) is responsible for destabilization of d_{z^2} orbital through interactions of σ-bonding.

III. PHOTOTHERMAL EFFECT

A. The fundamental photothermal mechanism in porphyrins

The photothermal effect is the physical manifestation of photon to thermal energy conversion through a material with an appreciable

FIG. 5. Porphyrin molecular orbitals (MO) relevant to the Gouterman four-orbital model. Symmetry nodes are drawn in dash lines.

absorption of light. Upon irradiation of various light sources, be it monochromatic or white light, the photothermal material can generate sufficient heat, thereby raising the local temperature within a short duration, provided that the material has considerable photothermal efficiency. The photothermal energy conversion for transition metals, especially those of nanoscale, is typically characterized by surface plasmon resonance (SPR). The photothermal effect has been extensively studied for gold and graphene, and the energy conversion is attributed to the localized surface plasmon resonance (LSPR).[21,62,63] A localized plasmon is the result of the confinement of a surface plasmon in a nanoparticle smaller than the wavelength of the incident light. A nanoparticle's response to the oscillating electric field can be described by the so-called dipole approximation of Mie theory.[64] The wavelength-dependent extinction cross section of a single particle defines the energy losses in the direction of propagation of the incident light due to both scattering and absorption.[21,62,63,65–67] However, Zhao et al. found a different photothermal mechanism for the porphyrin compounds that is associated with the porphyrin ring molecular structure based on Raman data (Fig. 7).[16]

Figure 7 shows the Raman spectra of the chlorophyll, chlorophyllin, hemoglobin, and phthalocyanine samples. Raman peaks are typically identified as molecular vibrations involving bonds of the porphyrins and can be significantly enhanced if the incident photon

energy is near the optical absorptions. Consistently, for 415 nm laser excitation, the Raman peaks are significantly enhanced for chlorophyll, chlorophyllin, and hemoglobin due to their absorption peaks near 400 nm, while those by the 514 nm laser are considerably reduced, indicating the strong associations between the photon absorptions and the porphyrin structures in these compounds. For phthalocyanine, the 633 nm laser results in much stronger Raman peaks corresponding to its absorptions in the NIR range. These results provide a physical base for the molecular oscillation-induced photothermal effects in the porphyrins.

B. Photothermal thin film deposition

Spin coating is an effective method for making uniform photothermal thin films of various kinds. The thickness of PT film can be well-controlled by rotational speed of spin processor and solution concentration. Zhao et al.[15] reported the multilayer chlorophyll PT films on a glass substrate via spin coating (Fig. 8) and found that both the photothermal effect and the average visible transmittance (AVT) are interrelated via the chlorophyll concentration which plays a key role in the single-pane window application. They also investigated the structures and properties of different porphyrin compounds such as chlorophyllin, hemoglobin, and phthalocyanine, and developed their thin
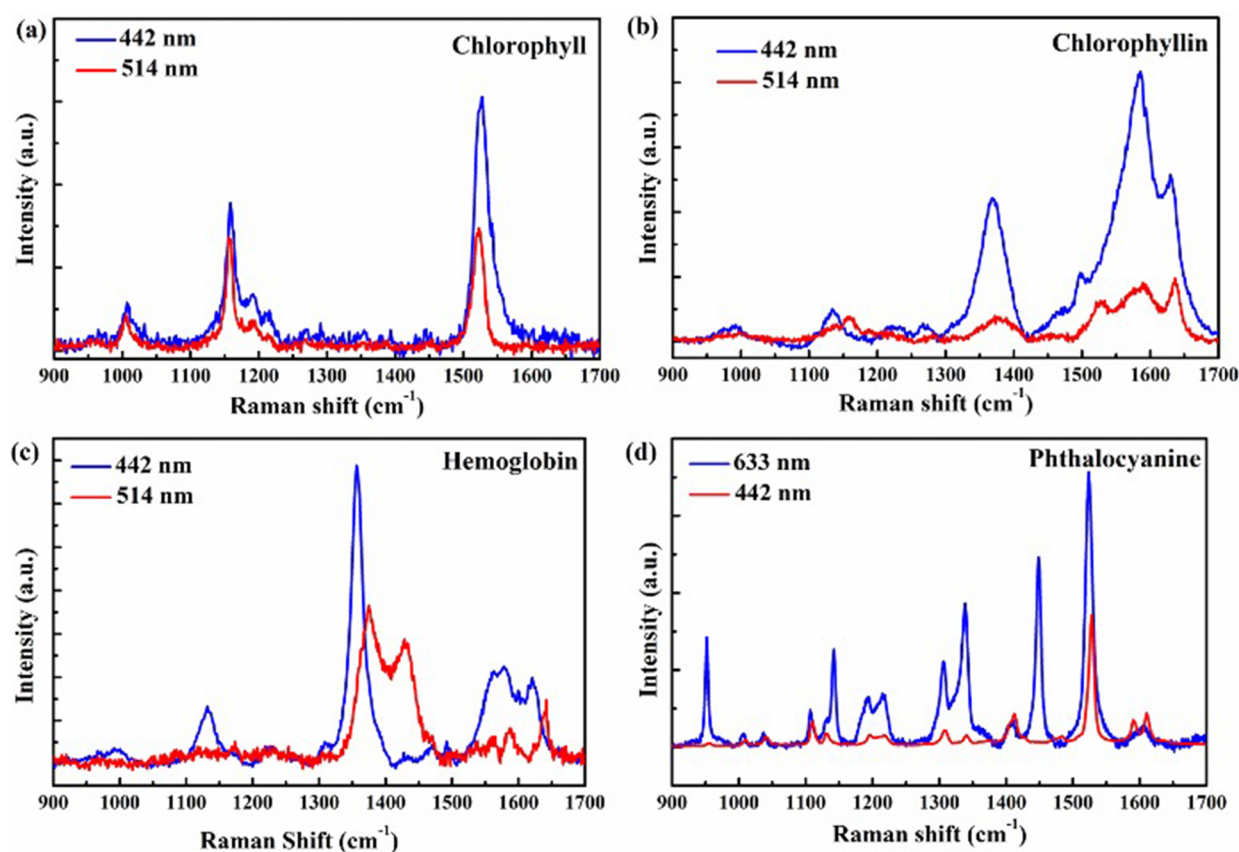

FIG. 7. Raman spectra of (a) chlorophyll, (b) chlorophyllin, (c) hemoglobin, and (d) phthalocyanine on aluminum foils, by 442, 514, and 633 nm lasers, respectively.[16] Reproduced with permission from Zhao et al., J. Phys. Chem. C **124**, 2 (2019). Copyright 2019 American Chemical Society.
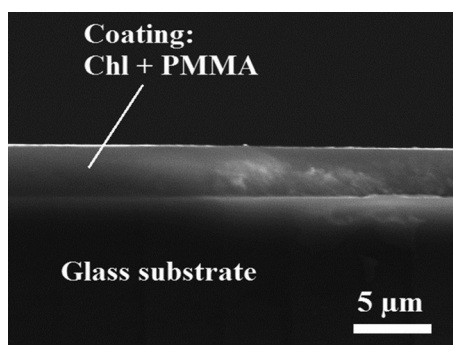
FIG. 8. SEM cross-sectional image of the four-layer chlorophyll (Chl) film with polymethyl methacrylate (PMMA) coated on glass substrate.[15]
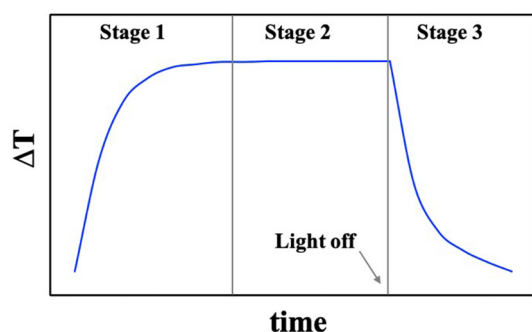

FIG. 9. Schematic diagram showing three stages in the temperature vs time curve.

films by spin-coating.[16] As shown in Fig. 3(c), the absorption of chlorophyllin (Chlin) is more pronounced than those of chlorophyll (Chl), hemoglobin (HB), and phthalocyanine (Phth) at the same concentration. Therefore, stronger photothermal effect is observed in the chlorophyllin thin films under the simulated solar light. They have also

calculated various parameters of the porphyrin thin films based on the heating/cooling curves including U-factor, photothermal conversion efficiency, specific absorption rate, and specific photothermal coefficient.[16]

C. The characteristics of the photothermal effect

Figure 9 schematically depicts the heating/cooling curve of a photothermal material under light irradiation. There are three stages in the temperature changed (ΔT) vs time plot: initial and rapid heating region (stage 1), steady state (stage 2), and cooling region (stage 3), respectively. Stage 1 indicates the heating of the sample due to the photothermal effect is greater than heat loss, thereby a rapid increase in temperature. In stage 2, the photothermal heating is balanced by the heat loss through the sample surface, causing a temperature plateau in this region. In other words, the heat loss of the sample is equal to the heat gain by the photothermal effect. At the beginning of stage 3, the light source is turned off, resulting in a Newtonian cooling behavior in this region.

The photothermal effect of the material is closely related to the optical absorption spectra and excitation photon energy. For laser excitation, more efficient photothermal effect can be generated if the incoming photon energy is near the high energy edge of the absorption peak. For white light irradiation, the photon harvesting takes a wide range of the absorption spectrum. Specifically, the B band and Q band of chlorophyll are at approximately 415 and 664 nm, respectively [Fig. 3(c)]. Figure 10 shows the relatively temperature differences of chlorophyll thin films and solution under 660 and 785 nm laser irradiation for 10 min. As can be seen in this figure, the temperature increase is much rapid by the 660 nm laser than that by the 785 nm laser due to the absorption peak near 660 nm. Therefore, to enhance both the photothermal effect and transparency, the material must be spectral selectively tailored via structural design and compositional optimization to achieve strong absorptions in the non-visible regions such as NIR and high average visible transmittance (AVT).

Figure 11(a) shows the relatively temperature differences of the multilayer chlorophyll thin films under white light irradiation. Consistently, thicker films (each layer is ~2 μm) give greater ΔT_g as
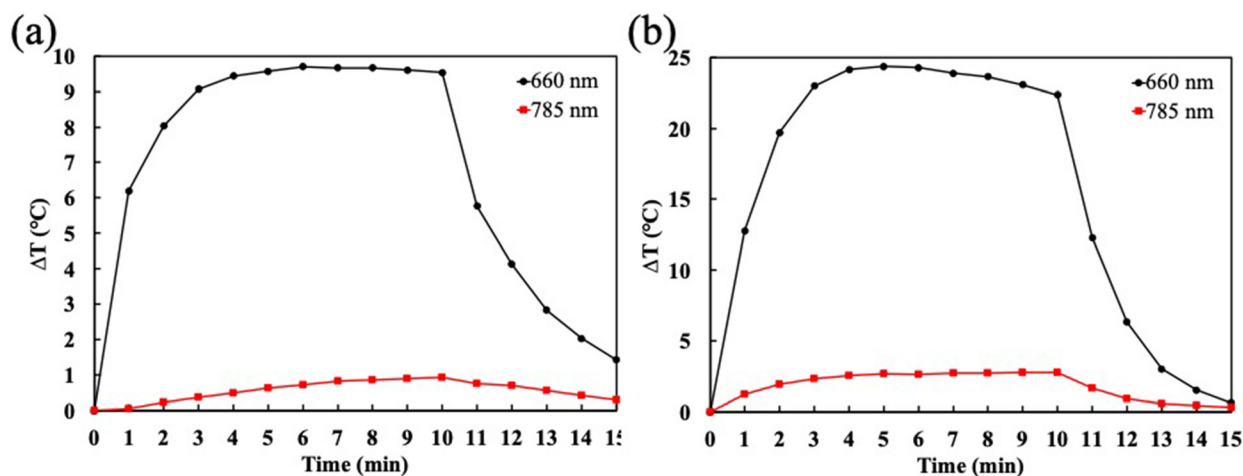

FIG. 10. ΔT_g vs time for (a) Chl in 1-butanol and (b) Chl-coated glass irradiated by 661 and 785 nm lasers.[15]

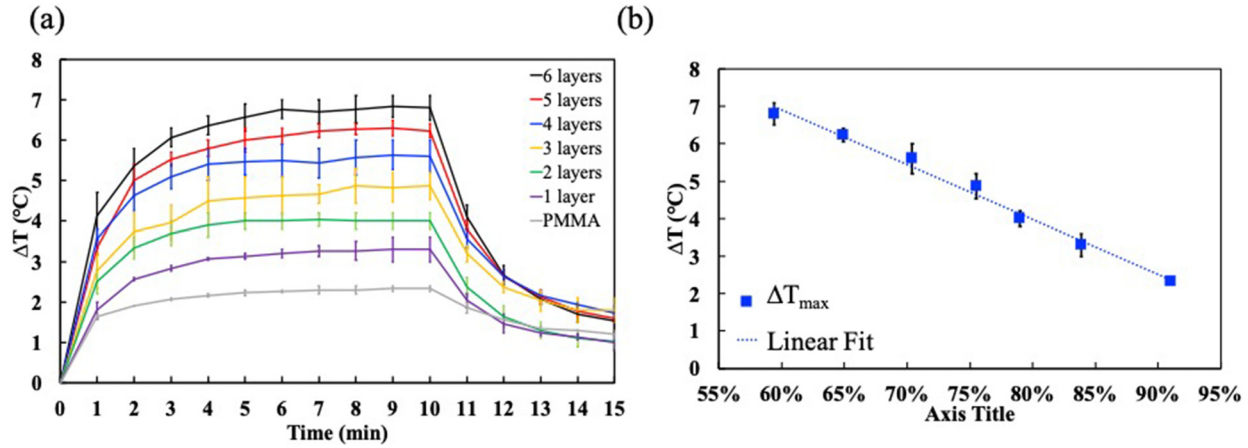FIG. 11. (a) ΔT_g vs time for different layers of chlorophyll coating irradiated by simulated solar light. (b) Linear $\Delta T_{g,\ max}$ vs average visible transmittance relationship of chlorophyll coating.[15]

expected, but lower visible transmittance. Figure 11(b) shows a linear relationship between $\Delta T_{g,max}$ vs visible transmittance for thin films of different layers. The same behaviors have been observed in other porphyrin compounds of chlorophyllin, hemoglobin, and phthalocyanine samples as shown in Fig. 12. The linear relationships between ΔT_{max} and AVT for all thin film samples indicate that the photothermal behavior is highly correlated with the optical transmittance and absorption.

1. Photothermal conversion efficiency (η)

The photothermal conversion efficiency, η, is defined as the ratio of the thermal energy generated by the sample to the incident photon energy. The photothermal conversion efficiency for solar light was developed by Jin et al.[68] and modified by Lin et al.[17]

$$\eta = \frac{(C_g m_g + C_{PT\ material}m_{PT\ material} + C_{polymer}m_{polymer})\Delta T_{max}}{IA\Delta t}$$

$$\approx \frac{C_g m_g \Delta T_{max}}{IA\ \Delta\ t} \times 100\%,\qquad(1)$$

where $\Delta T_{control}$ is the maximum change in temperature increase in the polymethyl methacrylate (PMMA) film without photothermal materials. This equation can be simplified as[15,17]

$$SAR = \frac{C_{glass}m_{glass}(\Delta T_{max} - \Delta T_{control})}{m_{PT\ material}\Delta t}.\qquad(3)$$

SAR is an important parameter that characterizes the materials' abilities in photon absorption. As is well-known, all materials and surfaces are capable of absorbing photon energy to certain degrees. However,

where g is glass, c is the specific heat capacity (J/g·°C), m is mass (g), ΔT_{max} is the maximum change in temperature increase in the sample (°C), I is the incident light power density (W/cm^2), A is the surface area of the sample, and Δt is the time required for a sample to reach the maximum temperature (s). The photothermal conversion efficiencies have been determined for various PT materials and thin films.[15,17] The biomedical applications of PT have been extensively studied mainly for medical therapeutics. In a typical medical PT therapeutics, both the quantity of the materials (~mg) and the total thermal energy required are significantly low for a highly localized tumor treatment.[1–8] However, in energy applications, the η value is more critical as the total thermal energy generated is much greater, compared to that of the medical therapeutics, considering the large surface area of the thin films, such as the building skin.

2. Specific absorption rate (SAR)

The specific absorption rate (SAR) of a photothermal material is a measure of the rate at which energy is absorbed by the material when exposed to an incident light and can be expressed as[15,17]

$$SAR = \frac{(C_{glass}m_{glass} + C_{PT\ material}m_{PT\ material} + C_{polymer}m_{polymer})\Delta T_{max} - (C_{glass}m_{glass} + C_{polymer}m_{polymer})\Delta T_{control}}{m_{PT\ material}\Delta t},\qquad(2)$$

in engineering applications, high SAR is required for rapid heat increase and pronounced photothermal effect for efficient energy conversion and heat generation.

3. Specific photothermal coefficient (SPC)

Specific photothermal coefficient is an intensive material characteristic that varies from system to system. For energy conversion studies, it is important to characterize a system with a material-specific
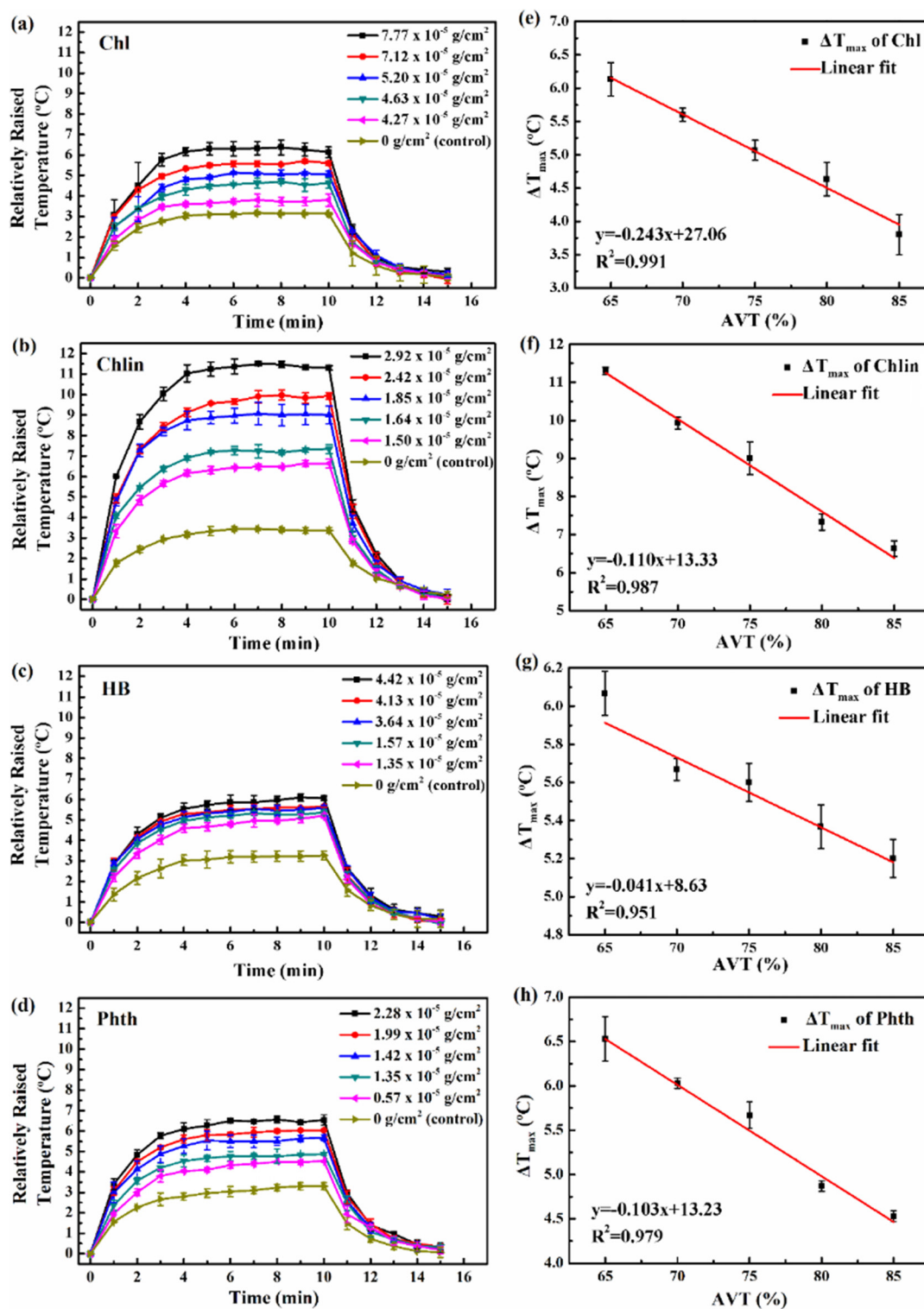
FIG. 12. Temperature difference ΔT vs time for (a) chlorophyll (Chl), (b) chlorophyllin (Chlin), (c) hemoglobin (HB), and (d) phthalocyanine (Phth) samples, with concentrations indicated; and ΔT_{max} vs AVT for (e) chlorophyll, (f) chlorophyllin, (g) hemoglobin, and (h) phthalocyanine samples. All samples are illuminated by simulated solar light (0.1 W/cm^2).[16] Reproduced with permission from Zhao *et al.*, J. Phys. Chem. C **124**, 2 (2019). Copyright 2019 American Chemical Society.

parameter, regardless of its volume and concentration. In this way, the intrinsic properties of the materials can be well-characterized for photon-to-heat conversion. Specific photothermal coefficient μ (SPC) is defined as the thermal energy produced/converted.[16] SPC can be expressed as[16]

$$SPC = \frac{\dot{Q}}{mass_{PT\ material}} \qquad (4)$$

where $\dot{Q}$ is the heat produced via photothermal effect in unit of time (J/s) and $mass_{PT\ material}$ is the mass of photothermal material.

SPC can be calculated based on the cooling curve in stage 3 as shown in Fig. 9. The SPCs of some porphyrin compounds have been reported[16] to be 129 J/g·s for the chlorophyll film, 619 J/g·s for the chlorophyllin film, 180 J/g·s for the hemoglobin film, and 352 J/g·s for the phthalocyanine film. The higher SPC value indicates the greater photon-to-heat conversion ability.

4. U-factor

The rate of heat loss by radiation, convection, and conduction through a medium is defined as U-factor. Since U-factor is essentially the thermal transmittance, the lower the U-factor, the better the thermal insulation. As a result of energy price increase, thermal insulation has become increasingly important for energy sustainability. According to the U.S. Advanced Research Projects Agency-Energy (ARPA-E),[69] the energy and element consumption of buildings can be improved by replacing the double-pane window with a single-pane, specifically for the cold climate area in the U.S. The general requirement of U-factor for window has been reported by NFRC[70] that the minimum requirement of U-factor is < 1.7 W/m^2 K although the U-factor requirement varies for different climate zones.[71] Hence, the reduction of U-factor is a critical criterion in building skin designs.

In accordance with ASTM C1199-14,[72] the general U-factor can be expressed as

$$U = \frac{1}{\dfrac{1}{h_h} + \dfrac{1}{h_c} + \dfrac{1}{U_L}}, \qquad (5)$$

where h_h and h_c represent the interior and exterior heat coefficients, and U_L is the heat transfer coefficient of the windowpane. The U-factor calculation should be modified for vary materials and climate conditions.[6,15–17] The U-factor equation can be expressed as[17]

$$U = \frac{1}{\left(\dfrac{T_{in} - T_{out}}{T_{in} - T_g}\right) \times \dfrac{1}{1.46 \times \left[\dfrac{(T_{in} - T_g)}{L}\right]^{0.25} + \sigma e \left[\dfrac{(T_{in}^4 - T_g^4)}{(T_{in} - T_g)}\right]} + \dfrac{1}{\sqrt{\left(0.84 \times (T_g - T_{out})^{\frac{1}{3}}\right)^2 + (2.38 \times v^{0.89})^2}}}, \qquad (6)$$

where T_{in} is the interior temperature, T_{out} is the exterior temperature, v is wind speed, L is the height of window, σ is Stefan–Boltzmann constant (5.67×10^{-8} W/m^2·K^4), e is the emissivity, and T_g is the inside surface temperature, respectively.

Equation (6) can be applied to evaluate the thermal insulation of a window with a temperature increase on the interior surface by photothermal coating. Based on Eq. (6), Lin *et al.*[17] estimated the U-factor of Fe$_3$O$_4$ and Fe$_3$O$_4$@Cu$_{2-x}$S films with the following parameters: T_{in}: 21.11 °C; T_{out}: −17.78 °C; v: 5.5 m/s; L: 1.50 m, and e: 0.84. Assuming the original interior window temperature is 5 °C, and T_g is calculated to be 278.15 K $+ \Delta T_{max}$. The U-factors of Fe$_3$O$_4$ and Fe$_3$O$_4$@Cu$_{2-x}$S films can be, respectively, reduced to 1.54 and 1.46 (W/m^2 K)[17] which are excellent values, all smaller than the minimum requirement of U-factor (<1.7 W/m^2 K) reported by NFRC.[70] Furthermore, Zhao *et al.*[15] reported a concept of multilayer chlorophyll (Chl) films for energy-efficient window application. By applying the chlorophyll photothermal coatings, they effectively lowered the U-factor of the single pane from 1.99 to 1.42 (W/m^2 K). These results indicate a high possibility of single-panes even in the cold climate areas via the solar-heated window surfaces based on the concept of optical thermal insulation without any interfering medium. The low U-factors obtained from these single-panes show promising potentials of the highly transparent, spectral selective thin films for optical thermal insulation.[15–17]

D. Biomedical applications of porphyrin compounds

The photothermal therapy (PTT) has been widely applied in biomedical areas especially in cancer therapeutics. If a PTT agent can be delivered to the tumor site via cell targeting, it results in effective cancer cell killing via sheer heat generated locally.[73,74] The cancer cells can be killed if the local temperature can reach $\sim$45 °C. However, most of the PTT replies on strong photothermal materials such as gold and graphene which pose significant toxicity and non-biodegradability. The bio-incompatibilities have raised considerable concerns in clinical applications. Porphyrin compounds are naturally occurring materials such as chlorophyll which is extracted from green vegetables. Not only are they environmentally green, but also non-toxic, making these green materials ideal for medical applications. The PTT typically employs the PT materials in the solution form which are delivered to the lesion sites via intravenous or direct injection. The photothermal heat is mainly generated by NIR band excitation using lasers for its deeper tissue penetration. The porphyrin compounds are known for their high packing density and photon absorption,[68] making them excellent photosensitizers in PTT. They have also been used for magnetic resonance imaging (MRI).[10,75–78] For instance, Mn-based porphyrin is a good MRI and PTT agent because Mn^{3+} ions can generate sharp contrast in MRI while exhibiting the photothermal effects after three serial treatments.[76] Su *et al.*[77] reported the porphyrin and

graphene oxide (GO) composite as a good photothermal therapeutic agent. Compared to using GO or porphyrin separately, the combination of GO and porphyrin has a broader light absorption region. Chu *et al.*[10] extracted chlorophyll from plants and encapsulated it into pluronic F68 (Plu) micelles for photothermal therapy and cancer imaging. Since chlorophyll can be extracted from most of the green vegetables, it is non-toxic and biocompatible; therefore, it is an attractive material for clinical applications.

IV. PHOTOVOLTAIC EFFECT OF PORPHYRIN COMPOUNDS

A. The fundamentals of photovoltaic effect

In solar light harvesting and energy conversion, photovoltaics is best known for converting energy from the sunlight to electricity and successfully applied for energy sustainability. However, the power conversion efficiency (PCE) of PVs varies widely from the silicon-based materials to polymers.[79] According to the chart of best research-cell efficiency from NREL,[79] the best efficiency of organic cell achieved 17.5% and the best efficiency of a multijunction cell can attain up to 47.1%. The most common polymer solar cells (PSC) are made of P3HT and PCBM ([6,6]-phenyl-C61-butyric acid methyl ester) polymers with PCE about 13%. Although this is quite far from the 20% efficiency of the commercial solar panels, PSC has the advantages of light weight, low price, flexible for applications in biomedicine, remote microwatt sensors, wireless appliances, and visually enhanced finesse for architectural designs and building materials.[80–83]

Structurally different from silicon-based inorganic PVs that involve the construction of a p–n junction, PSC typically utilizes conductive organic polymers for solar harvesting and charge transport to produce electricity by the photovoltaic effect. Most of the organic solar cells (OSC) are based on the polymers with the π electron system which is responsible for absorbing photons and transporting electrons by the conjugated π electrons. Light absorption leads to excitation of π electrons from the highest occupied molecular orbital (HOMO) to the lowest unoccupied molecular orbital (LUMO) of the molecule. The light absorbance wavelength can be determined by the energy bandgap between the HOMO and the LUMO.[84,85]

Charges are dissociated at the donor–acceptor interface by the dissociated driving force provided by the energy offset between the electron donor and electron acceptor. The basic working principle in a molecular-based device can be summarized as follows (Fig. 13): (1) exciton generation caused by light absorption; (2) exciton diffusion toward a donor–acceptor interface; (3) exciton dissociation at the interface and charge carrier transport, and (4) charge carrier collection at the external electrodes.[86]

B. The performance of a solar cell

The performance of the cells is determined by the current–voltage curves or I–V curves. The curve is obtained by the current and voltage of the cell measured through an external variable resistance under a standard intensity of incident light. The standard illumination for testing is 0.1 W/cm^2 (AM 1.5), which is the sunlight intensity reaching earth surface through air mass at a solar zenith angle of 42.8°. The main parameters are provided by I–V curves, such as the power conversion efficiency (PCE), open-circuit voltage (V_{OC}), short-circuit current (I_{SC}), and fill factor (F.F.) (Fig. 14).
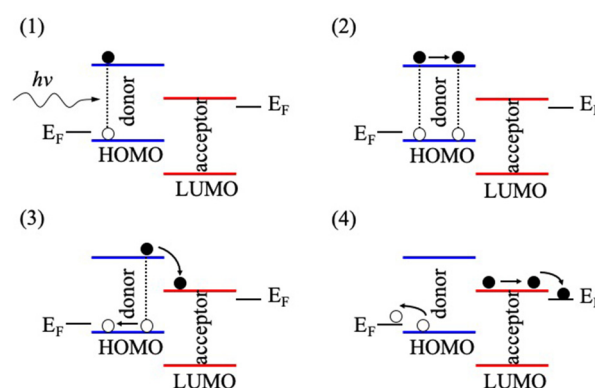
FIG. 13. The principles of charge separation in organic solar cell.[86]

1. Power conversion efficiency (PCE, η)

The power conversion efficiency is a parameter for representing the energy production of a solar cell. The efficiency can be calculated by the following equation:

$$\eta = \frac{P_{max}}{P_{in}} = \frac{I_{sc} \times V_{oc} \times F.F.}{P_{in}} \times 100\%, \tag{7}$$

where P_{max} is the maximum power per area (W/m^2), P_{in} is the light power per area (W/m^2), I_{SC} is the short circuit current (A), V_{OC} is the open circuit voltage (V), and F.F. is fill factor (%).

For ideal I–V curve, the maximum power per unit area can be expressed as

$$P_{max} = I_{max} \times V_{max}, \tag{8}$$

where I_{max} and V_{max} are voltage and current where the generated power is at the maximum.

Short circuit current (I_{SC}) is the highest current density obtained when there is no applied voltage. The short circuit current is affected by the driving force for electron injection into the conduction band from the excited dyes. The open-circuit voltage (V_{OC}) is the maximum

FIG. 14. Schematic of I–V curve.

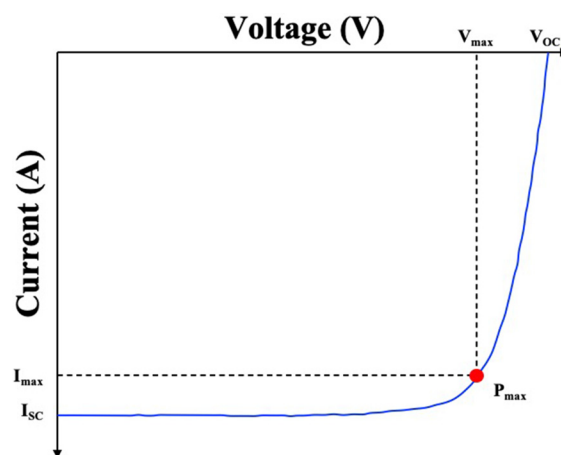voltage obtained at no current flow. It is determined that the V_{OC} will be increased by having lower driving force or more positive redox potential.[87] It corresponds to the energy difference between the Fermi level of the semiconductor and the redox couple's energy level. Fill factor (F.F.) is defined as a ratio of the maximum power to the product of its V_{OC} and I_{SC}, and it can be expressed as follows:

$$F.F. = \frac{I_{max} \times V_{max}}{I_{sc} \times V_{oc}} \times 100\%. \qquad (9)$$

2. Incident photon-to-current conversion efficiency (IPCE)

IPCE is an important parameter that presents the percentage of the absorbed light converted to current by a solar cell. IPCE indicates the spectral sensitivity of a solar cell by measuring intensity via a monochromatic light. IPCE can be expressed as

$$IPCE(\%) = \frac{1240 \times J_{sc}}{\lambda \times P_{in}} \times 100. \qquad (10)$$

Here, the J_{SC} is the short-circuit photocurrent density. The performance of dye-sensitized solar cells (DSSCs) is dependent on the characteristics of the individual components above. Many investigations focus on various materials parameters, such as substrate, photoanode,[88–92] dyes,[31–35] electrolyte,[84,85] and counter electrode.[86–91] Research also focuses on the structure—properties relationships of the individual components and interface effect on the performance of DSSCs.

3. Dye-sensitized solar cells (DSSCs)

The engineering issues of DSSCs such as stability of dye and leakage of electrolyte have been experimentally addressed for a variety of applications. A DSSC consists of photoanode, dyes, electrolyte, and counter electrode [Fig. 15(a)]. The working principle of DSSC can be described as follows [Fig. 15(b)]: (i) when the sunlight hits the device, the electrons in the dye molecules will be excited from ground state (HOMO) into excited state (LUMO); (ii) the excited dye molecules are oxidized (loss of electrons) and electrons are injected into the conduction band of the semiconductor; (iii) the oxidized dye molecules are regenerated by electron donation from the redox mediator (I^-), and two I^- are oxidized to iodine (I_3^-), and (iv) the I_3^- diffuses toward the counter electrode and then it is reduced to I^- by receiving electrons from counter electrode (cathode). Although the photon-to-electricity efficiency of DSSC is quite low, it has many advantages, including non-toxic, environmentally friendly, cost-efficient, simple manufacturing processes, etc.

The substrate for a DSSC is a transparent conductive oxide (TCO) glass, made of indium tin oxide (ITO) or fluorine-doped tin dioxide (FTO). Metal oxide semiconductors are used for making photoanode of DSSC, namely, TiO_2,[88] ZnO,[89] SnO_2,[90] and Nb_2O_5[91] for transporting the electrons, which is also called the electron transport layer. Two main semiconductors commonly used for DSSC are TiO_2 and ZnO, and the bandgap of both materials is 3.2 eV.[92] Electrolytes are an essential mediator between the photoanode and counter electrode in DSSC. Electrolyte regenerates the dye sensitizer from oxidized state back to ground (steady) state by gaining electrons from redox mediator.[84] The lost electrons are gained from the electrolyte, an operation known as redox reaction. For example, the oxidized dyes can be regenerated by the iodide species I^-. I^- loses electrons to dyes, resulting in formation of I_3^-. The triiodide can be returned by gaining electrons from counter electrode (cathode), and the reaction can be expressed as

$$I_3^- + 2e^- = 3I^-$$
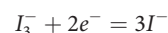
The efficiency of DSSCs depends on the kinetics of electron transfer at the liquid junction of the sensitized semiconductor/electrolyte interface. For effective devices, the electron injection rate should be faster than dye degradation rate.[85] However, there are some challenges for using metal-salt based liquid as electrolyte, in particular, difficulties in tandem architecture, poor sealing, and photodegradation, resulting in low lifetime and efficiency of a device. A sputtered platinum (Pt) is commonly used as a counter electrode in DSSC. The main
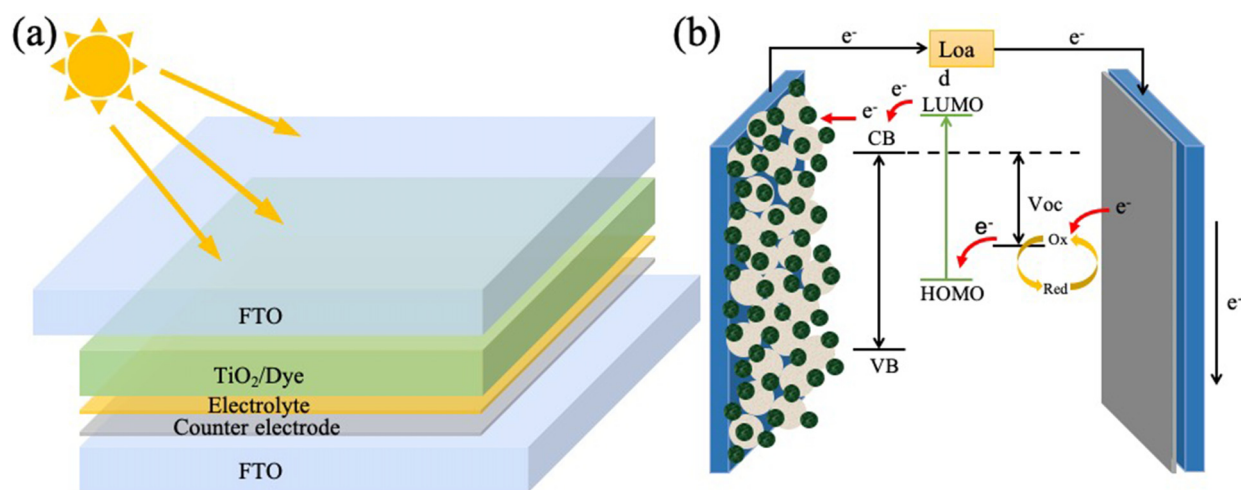

FIG. 15. (a) DSSC structure and (b) schematic working principle of DSSC.

purpose of the counter electrode is to catalyze reduction of I_3^- to I^- in redox electrolyte after electron injection. Since Pt is a rare and expensive metal, Pt-free counter electrodes are required to reduce the cost of DSSCs. Some alternative materials have been developed, for instance, transition metal compounds, carbon-based materials,[86,87] conducting polymers,[88,89] and composite materials.[90,91]

4. Porphyrin-based photosensitizer

Photosensitizers play a critical role in DSSC in producing the photo-induced electrons and injecting the electrons into the conduction band of the photoanode. The ideal photosensitizer should meet some requirements, particularly, wide light absorption range, good redox potential, high stability, and suitable anchoring property. Several groups have developed various porphyrin compounds as photosensitizers [Fig. 16(a)].[31–35,91–99]

Many porphyrin compounds have been used for developing solar energy conversion systems due to strong absorption in the visible region.[92–96] Kay and Gratzel[31] reported the first "porphyrin" DSSC based on many porphyrin complexes such as chlorophyll, chlorophyllin, pheophorbide, Zn-mesoporphyrin IX, etc. Porphyrin DSSC with Cu-2-α-oxymesoisochlorin attained a PCE of 2.6% in 1993,[31] which was further increased to 12.3% by using Zn(II)-porphyrin dye (YD2-o-C8) in 2011.[32] In 2014, a breakthrough efficiency of 13% for porphyrin based DSSC was obtained by utilizing Zn-porphyrin derivative (SM371).[33] The Zn(II)-porphyrin derivatives are used frequently for DSSC for its appreciable PCE.[97,98] In particular, Santos et al.[98] studied the differences between Zn-porphyrin and metal-free porphyrin, and found faster injection dynamics of Zn-porphyrin due to its more negative excited state oxidation potential than that of the metal-free porphyrins. Bessho et al.[99] investigated the photovoltaic effect of the Zn-porphyrin (YD-2), D205 dye, and YD-2/D205 cosensitizer. They found that the J_{sc} and PCE can be enhanced by using YD-2/D205 co-sensitizer for its improved light harvesting.

Other porphyrin compounds and its derivatives have also been investigated as photosensitizers, such as Mg(II)-porphyrin (chlorophyll),[31,93,95] Cu(II)-porphyrin (chlorophyllin),[31,100,101] Cu(II)-porphyrin (CuPc),[102,103] Ru-porphyrin (RuPc),[104] Ga-porphyrin (GaTsPc),[105] Fe-porphyrin (FeTsPc),[106] Ti-porphyrin (TiPc),[107] and metal-free porphyrin.[98,108] In comparison to Zn-porphyrins, PCE and stability of DSSC using other porphyrin compounds are, however, quite low. For instance, the PCE of the chlorophyll-based DSSC was reported to be only 0.73% by Amao and Komori in 2003.[109] Taya et al. improved the efficiency up to 1.077% in 2015.[110] Later on, Hassan and co-worker reported a PCE of chlorophyll-based DSSC about 2.62% in 2016.[111] Some studies indicated that PCE of chlorophyll-based DSSC can be improved by applying multiple dye[112,113] or doping metal.[114] Despite the low PCE, the major advantages of chlorophyll-based photosensitizers include its green nature, low-cost, and high light harvesting ability. There have been new strategies to enhance the light harvesting ability of the photosensitizer by using (i) push–pull porphyrins,[115,116] (ii) porphyrin dimers,[108,117] and (iii) multiple dyes.[97,118,119]

Push–pull (donor–acceptor) porphyrins are made of an electron-donating group (D), π-bridge (π), and an electron-withdrawing group (A). A π-bridge is the conjugation units connecting the donor and acceptor. The spectra and electron transfer can be determined by the electronic interaction between the D and A groups. The D-π-A group of photosensitizers determines the procedures in an operating DSSC, which are oxidized-dye regeneration and hot-electron injection. The donor group is considered the dye-regeneration reaction after electron injection, and the acceptor group is to deliver the electrons from photosensitizer to the semiconductor (e.g., TiO_2) for initiating the electron-hole separation process. Lee et al.[115] proposed a push–pull Zn porphyrin with strong electron-donating substituent and electron-
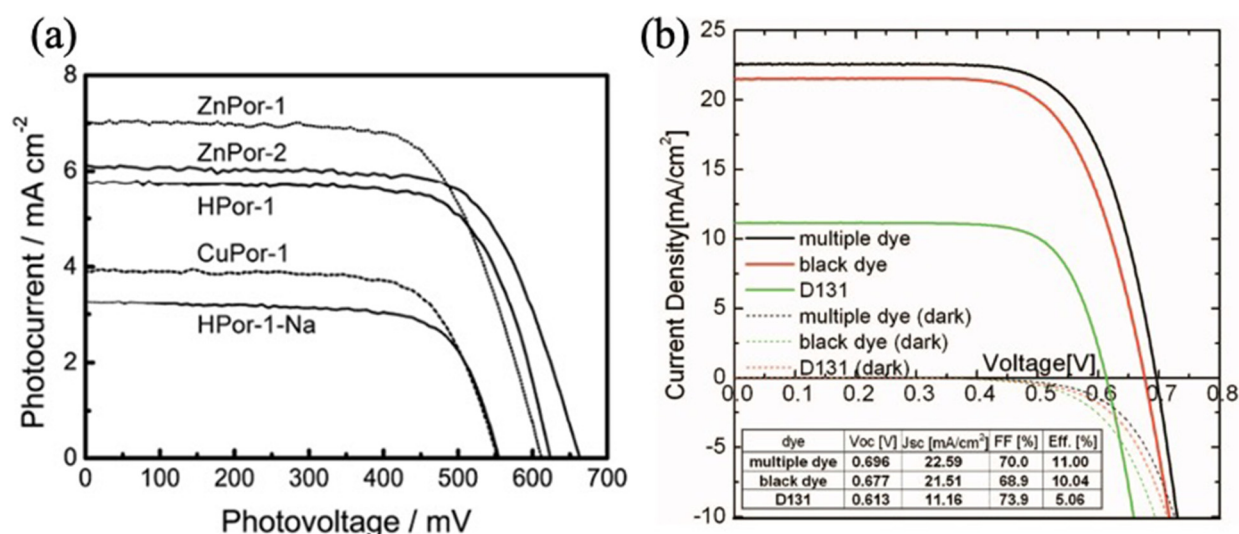
FIG. 16. PV performance of (a) porphyrin-sensitized solar cell.[91] Reproduced with permission from Wang and Kitao, Molecules **17**, 4 (2019). Copyright 2019 Multidisciplinary Digital Publishing Institute (MDPI); (b) multiple dyes (in black solid and dash lines) DSSC.[119] Reproduced with permission from Ogura et al., Appl. Phys. Lett. **94**(7), 073308 (2009). Copyright 2009 AIP Publishing. All J–V curves characterized under AM 1.5G illumination (1000 W/m²).

withdrawing substituent at meso-positions. They reported that por-phyrin's absorption bands with a phenylethynyl bridge are red-shifted and broadened due to extension of π-conjugation. The best PCE of Zn-porphyrin DSSC has so far reached 6%, which is competitive to the DSSC using the commercial dye (N3). Later, the performance of push–pull Zn porphyrin DSSC was improved by the same group,[116] and 7% PCE has been achieved.

A porphyrin dimer is to combine two porphyrin moieties by a chemical bond. Koehorst et al.[108] proposed a spectrally enhanced por-phyrin heterodimers DSSC. This research employed a covalently bonded Zn porphyrin (ZnP)/free base porphyrin (H$_2$P) heterodimers onto non-porous TiO$_2$ layers (H$_2$P-ZnP-TiO$_2$) on ITO (Indium Tin Oxide). They reported that the photocurrent is contributed by Zn por-phyrin dimer, resulting in faster energy transfer. In addition, Mozer et al.[117] proposed Zn–Zn porphyrin dimer (ZnP-ZnP) DSSCs and demonstrated that each porphyrin array contributes to current genera-tion in a cell. They found that the Soret band of dimers was broadened and the Q-bands showed a higher molar extinction coefficient than those of monomers. These results show the advantage of the porphyrin heterodimers in light harvesting.

Light harvesting of a DSSC device can also be enhanced by utiliz-ing multiple dyes. Otaka et al.[118] proposed the multicolored DSSCs with the red, purple, blue, green, and black color dyes in DSSCs. Ogura et al.[119] investigated a multiple dye system by applying terpyri-dine complex (black dye) and indoline dye (D131) in DSSC. They reported that the multiple dye system performs better IPCE than those with only black dye and showed an impressive light-to-electricity con-version efficiency (11%). They contributed this improved efficiency to the combination of multiple dyes that broaden the absorption spectra range for enhanced photon absorption [Fig. 16(b)].

V. PHOTOTHERMAL AND PHOTOVOLTAIC DUAL MODALITY

Some of the semiconducting materials exhibit both PT and PV effects. If designed appropriately, PT and PV dual modality is highly possible, specifically in some of the porphyrin compounds. The con-cept of PT–PV modality is schematically illustrated in Fig. 17. As shown in this figure, the PT–PV film is featured with several key char-acteristics: (1) it is highly transparent but only absorbing UV and NIR for energy conversion, which is particularly useful in building skin applications; (2) upon absorbing solar light in the UV and NIR regions, energy conversion seasonably takes two paths: photon-to-heat conversion in the winter for lowering the thermal transmittance and photon-to-electricity in warmer seasons as a solar panel; (3) the PT–PV dual modality can be switched easily by an electronic control unit depending upon the seasonal changes and energy needs, and (4) the PT and PV thin films can be integrated into the large-scale build-ing skin surface for effective solar harvesting that may compensate the low PCEs of the organic PVs. In the wintertime, the photothermal effect is utilized to heat the single-pane in order to reduce heat loss through the building skin based on optical thermal insulation. In this way, thermal insulation can be achieved optically without intervention medium. On the other hand, the undesirable solar infrared in summer can be compensated by the same thin film coating on the building skin but in a different modality: photovoltaic. Absorption of large infrared irradiation not only reduces cooling energy but generates elec-tricity for other appliances.
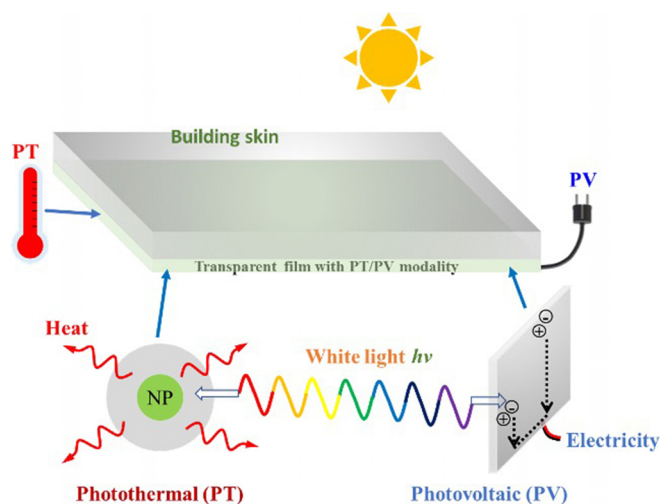

FIG. 17. Schematic of PT–PV modality based on transparent porphyrin compounds.

Ever since the discovery of the PV effect, a variety of material systems have been identified, synthesized, developed, and engi-neered into many different types of solar harvesting devices for energy applications.[120] These include Si-based solar cells, copper zinc tin sulfide (CZTS), perovskite solar cells (PSCs), dye-sensitized solar cells (DSSCs), etc. Among all DSSCs, the porphy-rin compounds have demonstrated the most attractive properties for photosensitizers.[30] Functionalization of macrocyclic dyes in the porphyrin compounds contributes to strong absorptions in the vis-ible light region.[28,29] The first application of porphyrin and its derivatives for DSSC was reported in 1993 by Kay and Gratzel.[31] They reported 2.6% of the overall photo-conversion efficiency (PCE) and attributed the low PCE to the Ohmic losses at high cur-rent densities. The PCE of Zn-porphyrin derivatives was increased up to 12.3% in 2011,[32] and further improved to 13% in 2014.[33] Although steady increase in PCE was achieved from 2009 to 2014,[34] challenging issues are to be addressed in the molecular design, particularly on the aging stability and inefficient photon collection in the Q band region (520 and >700 nm).[35] Overall, por-phyrin compounds have already been shown to have great poten-tial in developing advanced DSSCs by applying multiple dyes to extend light absorbing range for higher efficiency.[35]

In recent years, transparent PV and PT films have gained great attention for their high potentials in efficient solar harvesting and energy applications. The transparent organic photovoltaic (TOPV) thin films have been extensively studied.[121–123] Due to its high AVT, the so-called building integrated photovoltaic (BIPV) has been devel-oped for building skins taking the advantages of large surface areas without interfering with the color requirements.[83] It has been reported that efficiency of TOPV is about 6% while most of the commercial PVs ∼ 11%. To compensate this short coming in efficiency, the large surface area of building skin will be highly viable, specifically with PT–PV modality (or multimodality). Some of the porphyrin com-pounds are ideal material systems for PV–PT dual modality design as they are highly spectral-selective.

As described above, the common characteristics of both TOPV and transparent organic photothermal (TOPT) thin films are the strong UV and NIR absorptions for photon-to-electricity/thermal conversions. With these spectral selective features, the so-called building-integrated photovoltaics (BIPV) have been developed.[124–128] Yoon et al.[127] developed the amorphous silicon BIPV window (Fig. 18). They reported that the inclined and horizontal BIPV double windows' interior surface temperatures are about $2\,°C$ higher than that of the normal windows in winter. Moreover, Alrashidi et al.[128] studied the thermal performance of CdTe BIPV windows and compared its surface temperature with the single pane. They found the U-factor of CdTe BIPV is lower than the single glazing from indoor and outdoor experiments. Based on these results, the concept of PT–PV modality can be potentially applied in developing a multifunctional building skin as an active device, rather than a passive thermal barrier and lighting source. This concept will pave a new path to next generation device-based building skin with structures tailored to a variety of requirements in architectural and civic engineering in many areas, such as energy sustainability, environmental control, bio-medical assessment, public health, living comfort, utility efficiencies, and economic considerations.

VI. FUTURE PERSPECTIVES AND CONCLUSIONS

Sustainability is defined by the United Nations as "meeting the needs of the present without compromising the ability of future generations to meet their own needs." With advances in physics and materials science, it is possible to generate inexhaustible energy for meeting energy consumption forever. Presently, the renewability of energy relies on efficient harvesting of natural energy from sunlight, wind, rain, tides, waves, and geothermal heat.[129] Since solar energy is clean, sustainable, and plentiful, harvesting solar light has been a major approach in generating renewable energy for various applications such as generation of electricity, solar distillation, solar green houses, and solar heating of buildings.[130–133] In all solar-related technologies, novel

FIG. 18. Schematic diagram of building integrated photovoltaic (BIPV).

materials have played key roles in providing all required properties for solar harvesting, conversion, and energy generation. Currently, the research is extensively focusing on developing advanced materials with new properties that enable multifunctions in solar harvesting and energy generation. For significant solar harvesting, large-area panels are typically required, making building skins potentially viable substrates for both PT and PV panels. Both building-integrated photovoltaics (BIPV) and building-integrated photothermal (BIPT) systems are highly possible with the PT- and PV-dual modality designs. Advanced thin film technologies will enable both BIPV and BIPT to perform synergistically at the satisfactory level for sufficient energy saving and generation, seasonally altered and optimized. Recently, a study on the incident light angle dependence of the photothermal effect on several PT films has shown significance of the façade orientation and inclination angle for successful integration of PV and PT technologies.[18]

Although the silicon-based PV cells have achieved high conversion efficiency, there have been cost and environmental concerns in the manufacturing of the solar cells. It has been estimated that the solar energy costs approximately 8–10 times more than primary fuels ($\sim$\$0.38 per kilowatt hour for solar, $\sim$\$0.03 per kilowatt hour for gas).[134] The single largest cost is the solar panels themselves. Production of silicon PV panels is not "clean" as the by-product silicon tetrachloride can be both occupational and environmentally hazardous.[135–137] Porphyrin compounds exhibit both the PT and PV effects with significant AVT in the thin film form. They are also abundant in nature, environmentally friendly, and can be readily synthesized in laboratory straightforwardly and economically, making them highly desirable for both PV and PT applications.

The photothermal effects of nanoparticles have been previously investigated via laser excitations and mainly utilized for medical therapy.[6,7,39–41,73–78] Several nanoparticle systems are well-known for pronounced photothermal effects, such as gold and graphene. These nanoparticles, even in extremely small quantities of milligrams in solutions, all exhibit strong photothermal effects, effectively raising the solution temperature by greater than $30\,°C$ under laser excitations. However, most of the photothermal materials have not been experimentally investigated in the thin film forms for energy applications. Furthermore, few studies have been carried out on the photothermal effects of the metallic materials under white light excitations. Characteristically, most of the metallic materials are non-transparent with strong absorptions in the visible region. Porphyrin and its derivatives meet the transparency requirement by exhibiting selective absorptions only in the ultraviolet (Soret bands) and visible (Q bands) regions. The absorption spectra of porphyrins can be further selectively enhanced by modifying the conjugation and symmetry, substituents, substituted positions, and ligands. With these unique characteristics, new strategies have been proposed and experimentally carried out to enhance the light harvesting ability in DSSCs, such as push–pull porphyrins by utilizing porphyrin dimers, or applying multiple dyes. Some of these studies have shown a broadened spectrum with red-shifted via push–pull porphyrins, resulting in an amplified molar extinction coefficient. Therefore, combinations of specific porphyrins can be optimized for enhanced solar harvesting and utilized for PT and PV dual modality designs. The current research outcomes on the porphyrin compounds indicate their tremendous potentials in energy applications. The unique properties of porphyrin compounds
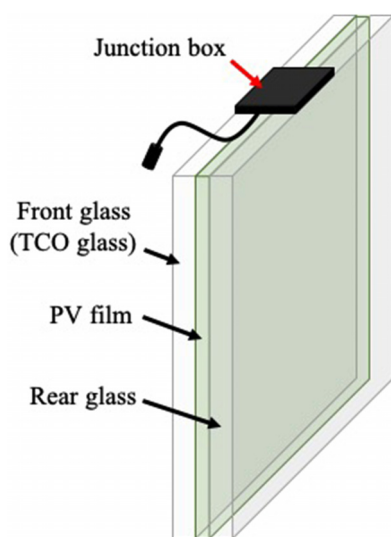
can be further utilized via large surface area of building skins for solar energy harvesting, conversion, and generation for next generation energy free systems.

ACKNOWLEDGMENTS

DATA AVAILABILITY

Data sharing is not applicable to this article as no new data were created or analyzed in this study.

REFERENCES

[1]M. I. Khot, H. Andrew, H. S. Svavarsdottir, G. Armstrong, A. J. Quyna, and D. G. Jaynea, "A review on the scope of photothermal therapy-based nanomedicines in pre-clinical models of colorectal cancer," Clin. Colorectal Cancer **18**(2), e200–e209 (2019).

[2]T. Pham, J. B. Jackson, N. J. Halas, and T. R. Lee, "Preparation and characterization of gold nanoshells coated with self-assembled monolayers," Langmuir **18**(12), 4915–4920 (2002).

[3]P. K. Jain, X. Huang, I. H. El-Sayed, and M. A. El-Sayed, "Noble metals on the nanoscale: Optical and photothermal properties and some applications in imaging, sensing, biology, and medicine," Acc. Chem. Res. **41**(12), 1578–1586 (2008).

[4]H. K. Moon, S. H. Lee, and H. C. Choi, "*In vivo* near-infrared mediated tumor destruction by photothermal effect of carbon nanotubes," ACS Nano **3**(11), 3707–3713 (2009).

[5]J. T. Robinson, S. M. Tabakman, Y. Liang, H. Wang, H. Sanchez Casalongue, D. Vinh, and H. Dai, "Ultrasmall reduced graphene oxide with high near-infrared absorbance for photothermal therapy," J. Am. Chem. Soc. **133**(17), 6825–6831 (2011).

[6]Y. Zhao, M. E. Sadat, A. Dunn, H. Xu, C. H. Chen, W. Nakasuga, R. C. Ewing, and D. Shi, "Photothermal effect on Fe_3O_4 nanoparticles irradiated by white-light for energy-efficient window applications," Sol. Energy Mater. Sol. Cells **161**, 247–254 (2017).

[7]Y. Zhao, A. Dunn, J. Lin, and D. Shi, "Photothermal effect of nanomaterials for efficient energy applications," in *Novel Nanomaterials for Biomedical, Environmental and Energy Applications* (Elsevier, 2019), pp. 415–434.

[8]Y. Lyu, Y. Fang, Q. Miao, X. Zhen, D. Ding, and K. Pu, "Intraparticle molecular orbital engineering of semiconducting polymer nanoparticles as amplified theranostics for *in vivo* photoacoustic imaging and photothermal therapy," ACS Nano **10**(4), 4472–4481 (2016).

[9]Y. Lyu, C. Xie, S. A. Chechetka, E. Miyako, and K. Pu, "Semiconducting polymer nanobioconjugates for targeted photothermal activation of neurons," J. Am. Chem. Soc. **138**(29), 9049–9052 (2016).

[10]M. Chu, H. Li, Q. Wu, F. Wo, and D. Shi, "Pluronic-encapsulated natural chlorophyll nanocomposites for *in vivo* cancer imaging and photothermal/photodynamic therapies," Biomaterials **35**(29), 8357–8373 (2014).

[11]S. K. Pushpan, S. Venkatraman, V. G. Anand, J. Sankar, D. Parmeswaran, S. Ganesan, and T. K. Chandrashekar, "Porphyrins in photodynamic therapy-a search for ideal photosensitizers," Curr. Med. Chem.-Anti-Cancer Agents **2**(2), 187–207 (2002).

[12]J. Kou, D. Dou, and L. Yang, "Porphyrin photosensitizers in photodynamic therapy and its applications," Oncotarget **8**(46), 81591–81603 (2017).

[13]B. Guo, G. Feng, P. N. Manghnani, X. Cai, J. Liu, W. Wu, S. Xu, X. Cheng, C. Teh, and B. Liu, "A porphyrin-based conjugated polymer for highly efficient *in vitro* and *in vivo* photothermal therapy," Small **12**, 6243–6254 (2016).

[14]Q. Zou, M. Abbas, L. Zhao, S. Li, G. Shen, and X. Yan, "Biological photothermal nanodots based on self-assembly of peptide–porphyrin conjugates for antitumor therapy," J. Am. Chem. Soc. **139**(5), 1921–1927 (2017).

[15]Y. Zhao, A. Dunn, and D. Shi, "Effective reduction of building heat loss without insulation materials via the photothermal effect of a chlorophyll thin film coated 'Green Window'," MRS Commun. **9**(2), 675–681 (2019).

[16]Y. Zhao, J. Lin, D. M. Kundrat, M. Bonmarin, J. Krupczak, S. V. Thomas, M. Lyu, and D. Shi, "Photonically-activated molecular excitations for thermal energy conversion in porphyrinic compounds," J. Phys. Chem. C **124**(2), 1575–1584 (2019).

[17]J. Lin, Y. Zhao, and D. Shi, "Optical thermal insulation via the photothermal effects of Fe_3O_4 and $Fe_3O_4@Cu_{2-x}S$ thin films for energy-efficient single-pane windows," MRS Commun. **10**(1), 155–163 (2020).

[18]M. Lyu, J. Lin, J. Krupczak, and D. Shi, "Light angle dependence of photothermal properties in oxide and porphyrin thin films for energy-efficient window applications," MRS Commun. **10**(3), 439–448 (2020).

[19]J. J. Wang and D. Shi, "Spectral selective and photothermal nano structured thin films for energy efficient windows," Appl. Energy **208**, 83–96 (2017).

[20]See https://solar.gwu.edu/how-much-land-would-it-take-power-us-solar for "How much land would it take to power the U.S. with solar?" (last accessed October 29, 2020).

[21]Fondriest Environmental, Inc., *Solar Radiation and Photosynthetically Active Radiation* (Fondriest Environmental, Inc., 2014).

[22]ASTM International, *Standard Tables for Reference Solar Spectral Irradiances: Direct Normal and Hemispherical on 37° Tilted Surface* (ASTM International, West Conshohocken, Pennsylvania, 2012), No. ASTM G173-03.

[23]G. Layer, D. Jahn, E. Deery, A. D. Lawrence, and M. J. Warren, "Biosynthesis of heme and vitamin B12," Compr. Nat. Prod. II **7**, 445–499 (2010).

[24]D. Sarkar, A. Sharma, and G. Talukder, "Chlorophyll and chlorophyllin as modifiers of genotoxic effects," Mutat. Res./Rev. Genet. Toxicol. **318**(3), 239–247 (1994).

[25]M. Gouterman, "Spectra of porphyrins," J. Mol. Spectrosc. **6**, 138–163 (1961).

[26]P. A. Lewis, "Colored organic pigments," *The Gardner Sward Handbook: Paint and Coating Testing Manual* (ASTM International, 1995), Vol. **17**, p. 190.

[27]H. Yin, S. Chen, S. H. Cheung, H. W. Li, Y. Xie, S. W. Tsang, X. Zhu, and S. K. So, "Porphyrin-based thick-film bulk-heterojunction solar cells for indoor light harvesting," J. Mater. Chem. C **6**(34), 9111–9118 (2018).

[28]K. Zeng, Z. Tong, L. Ma, W. H. Zhu, W. Wu, and Y. Xie, "Molecular engineering strategies for fabricating efficient porphyrin-based dye-sensitized solar cells," Energy Environ. Sci. **13**, 1617 (2020).

[29]A. J. Pistner, G. P. Yap, and J. Rosenthal, "A tetrapyrrole macrocycle displaying a multielectron redox chemistry and tunable absorbance profile," J. Phys. Chem. C **116**(32), 16918–16924 (2012).

[30]B. O'Regan and M. Grätzel, "A low-cost, high-efficiency solar cell based on dye-sensitized colloidal TiO_2 films," Nature **353**, 737–740 (1991).

[31]A. Kay and M. Grätzel, "Artificial photosynthesis. 1. Photosensitization of titania solar cells with chlorophyll derivatives and related natural porphyrins," J. Phys. Chem. **97**(23), 6272–6277 (1993).

[32]A. Yella, H. W. Lee, H. N. Tsao, C. Yi, A. K. Chandiran, M. K. Nazeeruddin, E. W.-G. Diau, C.-Y. Yeh, S. M. Zakeeruddin, and M. Grätzel, "Porphyrin-sensitized solar cells with cobalt (II/III)–based redox electrolyte exceed 12 percent efficiency," Science **334**(6056), 629–634 (2011).

[33]S. Mathew, A. Yella, P. Gao, R. Humphry-Baker, B. Curchod, N. Ashari-Astani, I. Tavernelli, U. Rothlisberger, M. K. Nazeeruddin, and M. Grätzel, "Dye-sensitized solar cells with 13% efficiency achieved through the molecular engineering of porphyrin sensitizers," Nat. Chem. **6**(3), 242–247 (2014).

[34]J. Lu, S. Liu, and M. Wang, "Push-pull zinc porphyrins as light-harvesters for efficient dye-sensitized solar cells," Front. Chem. **6**, 541 (2018).

[35]W. Li, M. Elkhaklifa, and H. He, "Design, engineering, and evaluation of porphyrins for dye-sensitized solar cells," in *Nanostructured Materials for Next-Generation Energy Storage and Conversion* (Springer, Berlin, Heidelberg, 2019), pp. 351–381.

[36]R. Lemberg, "Porphyrins in nature," in *Fortschritte der Chemie Organischer Naturstoffe/Progress in the Chemistry of Organic Natural Products/Progrés dans la Chimie des Substances Organiques Naturelles*, edited by L. Zechmeister (Springer, Vienna, 1954), Vol. 11.

[37]A. K. Arof and T. L. Ping, *Chlorophyll as Photosensitizer in Dye-Sensitized Solar Cells* (InTech, 2017).

[38]D. Dolphin, Z. Muljiani, K. Rousseau, D. C. Borg, J. Fajer, and R. H. Felton, "The chemistry of porphyrin π-cations," Ann. New York Acad. Sci. **206**(1), 177–200 (1973).

[39]M. J. Duffy, O. Planas, A. Faust, T. Vogl, S. Hermann, M. Schäfers, S. Nonell, and C. A. Strassert, "Towards optimized naphthalocyanines as sonochromes for photoacoustic imaging *in vivo*," Photoacoustics **9**, 49–61 (2018).

[40]M. Camerin, S. Rello, A. Villanueva, X. Ping, M. E. Kenney, M. A. Rodgers, and G. Jori, "Photothermal sensitisation as a novel therapeutic approach for tumours: Studies at the cellular and animal level," Eur. J. Cancer **41**(8), 1203–1212 (2005).

[41]H. Huang, W. Song, J. Rieffel, and J. F. Lovell, "Emerging applications of porphyrins in photomedicine," Front. Phys. **3**, 23 (2015).

[42]R. W. Wagner and J. S. Lindsey, "A molecular photonic wire," J. Am. Chem. Soc. **116**(21), 9759–9760 (1994).

[43]M. R. Wang and B. M. Hoffman, "Systematic trends in metalloporphyrin optical spectra," J. Am. Chem. Soc. **106**(15), 4235–4240 (1984).

[44]R. Syafinar, N. Gomesh, M. Irwanto, M. Fareq, and Y. M. Irwan, "Chlorophyll pigments as nature based dye for dye-sensitized solar cell (DSSC)," Energy Proc. **79**, 896–902 (2015).

[45]S. L. Bailey and P. Hambright, "Kinetics of the reactions of divalent copper, zinc, cobalt, and nickel with a deformed water soluble centrally monoprotic porphyrin," Inorg. Chim. Acta **344**, 43–48 (2003).

[46]N. B. Neto, D. S. Correa, L. De Boni, G. G. Parra, L. Misoguti, C. R. Mendonça, I. E. Borissevitch, S. C. Zílio, and P. J. Gonçalves, "Excited states absorption spectra of porphyrins–solvent effects," Chem. Phys. Lett. **587**, 118–123 (2013).

[47]D. Sundholm, "Density functional theory study of the electronic absorption spectrum of Mg-porphyrin and Mg-etioporphyrin-I," Chem. Phys. Lett. **317**(3–5), 392–399 (2000).

[48]D. Dolphin, *The Porphyrins* (Academica Press, New York, 1978), Vol. I–VII.

[49]R. Giovannetti, "The use of spectrophotometry UV-Vis for the study of porphyrins," Macro Nano Spectrosc. **1**, 87–108 (2012).

[50]P. Bhyrappa and P. Bhavana, "Meso-tetrathienylporphyrins: Electrochemical and axial ligation properties," Chem. Phys. Lett. **349**(5–6), 399–404 (2001).

[51]F. A. Walker and U. Simonis, "Iron porphyrin chemistry," *Encyclopedia of Inorganic Chemistry* (Wiley, 2006).

[52]P. Rothemund, "Formation of porphyrins from pyrrole and aldehydes," J. Am. Chem. Soc. **57**(10), 2010–2011 (1935).

[53]P. Rothemund, "A new porphyrin synthesis. The synthesis of porphin," J. Am. Chem. Soc. **58**(4), 625–627 (1936).

[54]A. D. Adler, F. R. Longo, J. D. Finarelli, J. Goldmacher, J. Assour, and L. Korsakoff, "A simplified synthesis for meso-tetraphenylporphine," J. Org. Chem. **32**, 476 (1967).

[55]C. H. Lee and J. S. Lindsey, "One-flask synthesis of meso-substituted dipyrromethanes and their application in the synthesis of trans-substituted porphyrin building blocks," Tetrahedron **50**(39), 11427–11440 (1994).

[56]A. Boudif and M. Momenteau, "Synthesis of a porphyrin-2, 3-diacrylic acid using a new '3+ 1' type procedure," J. Chem. Soc. Chem. Commun. **1994**(18), 2069–2070.

[57]J. S. Lindsey, I. C. Schreiman, H. C. Hsu, P. C. Kearney, and A. M. Marguerettaz, "Rothemund and Adler-Longo reactions revisited: Synthesis of tetraphenylporphyrins under equilibrium conditions," J. Org. Chem. **52**(5), 827–836 (1987).

[58]L. T. Nguyen, M. O. Senge, and K. M. Smith, "Simple methodology for syntheses of porphyrins possessing multiple peripheral substituents with an element of symmetry," J. Org. Chem. **61**(3), 998–1003 (1996).

[59]*Porphyrins and Metalloporphyrins*, edited by K. M. Smith (Elsevier, Amsterdam, 1975), Vol. 9.

[60]J. A. Shelnutt and V. Ortiz, "Substituent effects on the electronic structure of metalloporphyrins: A quantitative analysis in terms of four-orbital-model parameters," J. Phys. Chem. **89**(22), 4733–4739 (1985).

[61]M. S. Liao and S. Scheiner, "Electronic structure and bonding in metal phthalocyanines, metal'Fe, Co, Ni, Cu, Zn, Mg," J. Chem. Phys. **114**(22), 9780–9791 (2001).

[62]A. Rafiee and K. R. Khalilpour, "Renewable hybridization of oil and gas supply chains," in *Polygeneration with Polystorage for Chemical and Energy Hubs* (Academic Press, 2019), pp. 331–372.

[63]G. W. Crabtree and N. S. Lewis, "Solar energy conversion," Phys. Today **60**(3), 37–42 (2007).

[64]M. H. Chowdhury, K. Ray, and J. R. Lakowicz, "The use of aluminum nanostructures in plasmon-controlled fluorescence applications in the ultraviolet toward the label-free detection of biomolecules," Compr. Nanosci. Technol. **4**, 215–255 (2011).

[65]X. Huang, P. K. Jain, I. H. El-Sayed, and M. A. El-Sayed, "Plasmonic photothermal therapy (PPTT) using gold nanoparticles," Lasers Med. Sci. **23**(3), 217 (2008).

[66]M. E. Sadat, M. Kaveh Baghbador, A. W. Dunn, H. P. Wagner, R. C. Ewing, J. Zhang, H. Xu, G. M. Pauletti, D. B. Mast, and D. Shi, "Photoluminescence and photothermal effect of Fe_3O_4 nanoparticles for medical imaging and therapy," Appl. Phys. Lett. **105**(9), 091903 (2014).

[67]M. Scheffler, M. Dressel, M. Jourdan, and H. Adrian, "Extremely slow Drude relaxation of correlated electrons," Nature **438**(7071), 1135–1137 (2005).

[68]H. Jin, G. Lin, L. Bai, M. Amjad, E. P. Bandarra Filho, and D. Wen, "Photothermal conversion efficiency of nanofluids: An experimental and numerical study," Sol. Energy **139**, 278–289 (2016).

[69]ARPA-E, *Single-Pan Highly Insulating Efficient Lucid Designs (SHIELD) Program Overview* (ARPA-E, 2014).

[70]National Fenestration Rating Council, Incorporated, *Procedure for Determining Fenestration Product U-factors* (National Fenestration Rating Council, Incorporated, 2020), No. ANSI/NFRC 100-2017; last accessed July 18, 2020.

[71]See https://www.energystar.gov/products/building_products/residential_windows_doors_and_skylights/key_product_criteria#performance for criteria for "ENERGY STAR Program Requirements for Residential Windows, Doors, and Skylights" (last accessed July 18, 2020).

[72]*Standard Test Method for Measuring the Steady-State Thermal Transmittance of Fenestration Systems Using Hot Box Methods* (ASTM International, West Conshohocken, PA, 2014), No. ASTM C1199-14, see www.astm.org

[73]K. Yang, S. Zhang, G. Zhang, X. Sun, S. T. Lee, and Z. Liu, "Graphene in mice: Ultrahigh *in vivo* tumor uptake and efficient photothermal therapy," Nano Lett. **10**(9), 3318–3323 (2010).

[74]X. Huang, I. H. El-Sayed, W. Qian, and M. A. El-Sayed, "Cancer cell imaging and photothermal therapy in the near-infrared region by using gold nanorods," J. Am. Chem. Soc. **128**(6), 2115–2120 (2006).

[75]X. Song, Q. Chen, and Z. Liu, "Recent advances in the development of organic photothermal nano-agents," Nano Res. **8**(2), 340–354 (2015).

[76]T. D. MacDonald, T. W. Liu, and G. Zheng, "An MRI-sensitive, non-photobleachable porphysome photothermal agent," Angew. Chem. **126**(27), 7076–7079 (2014).

[77]S. Su, J. Wang, J. Wei, R. Martínez-Zaguilán, J. Qiu, and S. Wang, "Efficient photothermal therapy of brain cancer through porphyrin functionalized graphene oxide," New J. Chem. **39**(7), 5743–5749 (2015).

[78]H. S. Jung, P. Verwilst, A. Sharma, J. Shin, J. L. Sessler, and J. S. Kim, "Organic molecule-based photothermal agents: An expanding photothermal therapy universe," Chem. Soc. Rev. **47**(7), 2280–2297 (2018).

[79]See https://www.nrel.gov/pv/assets/pdfs/best-research-cell-efficiencies.20190802.pdf for "Best Research-Cell Efficiencies" (last accessed November 21, 2020).

[80]W. Y. Wong, X. Z. Wang, Z. He, A. B. Djurišić, C. T. Yip, K. Y. Cheung, H. Wang, C. S. Mak, and W. K. Chan, "Metallated conjugated polymers as a new avenue towards high-efficiency polymer solar cells," Nat. Mater. **6**, 521–527 (2007).

[81]S. Y. Chang, P. Cheng, G. Li, and Y. Yang, "Transparent polymer photovoltaics for solar energy harvesting and beyond," Joule **2**(6), 1039–1054 (2018).

[82]C. C. Chen, L. Dou, R. Zhu, C. H. Chung, T. B. Song, Y. B. Zheng, S. Hawks, G. Li, P. S. Weiss, and Y. Yang, "Visibly transparent polymer solar cells produced by solution processing," ACS Nano **6**(8), 7185–7190 (2012).

[83]C. J. Traverse, R. Pandey, M. C. Barr, and R. R. Lunt, "Emergence of highly transparent photovoltaics for distributed applications," Nat. Energy **2**(11), 849–860 (2017).

[84]L. Hojatkashani, "Theoretical investigation of application of combining pristine C_{60} and doped C_{60} with silicon and germanium atoms for solar cells; A DFT study," Orient. J. Chem. **35**(1), 255–263 (2019).

[85]I. Arbouch, Y. Karzazi, and B. Hammouti, "Organic photovoltaic cells: Operating principles, recent developments and current challenges–review," Phys. Chem. News **72**, 73–84 (2014).

[86]Y. J. Cheng, S. H. Yang, and C. S. Hsu, "Synthesis of conjugated polymers for organic solar cell applications," Chem. Rev. **109**(11), 5868–5923 (2009).

[87]A. Jena, S. P. Mohanty, P. Kumar, J. Naduvath, V. Gondane, P. Lekha, J. Das, H. K. Narula, S. Mallick, and P. Bhargava, "Dye sensitized solar cells: A review," Trans. Indian Ceram. Soc. **71**(1), 1–16 (2012).

[88]M. Singh, R. Kurchania, R. J. Ball, and G. D. Sharma, "Efficiency enhancement in dye sensitized solar cells through step wise cosensitization of TiO$_2$ electrode with N719 and metal free dye," Indian J. Pure Appl. Phys. **54**, 656–664 (2016), see http://nopr.niscair.res.in/bitstream/123456789/35896/1/IJPAP%2054(10)%20656-664.pdf

[89]M. Quintana, T. Edvinsson, A. Hagfeldt, and G. Boschloo, "Comparison of dye-sensitized ZnO and TiO$_2$ solar cells: Studies of charge transport and carrier lifetime," J. Phys. Chem. C **111**(2), 1035–1041 (2007).

[90]S. Gubbala, V. Chakrapani, V. Kumar, and M. K. Sunkara, "Band-edge engineered hybrid structures for dye-sensitized solar cells based on SnO$_2$ nanowires," Adv. Funct. Mater. **18**(16), 2411–2418 (2008).

[91]X. F. Wang and O. Kitao, "Natural chlorophyll-related porphyrins and chlorins for dye-sensitized solar cells," Molecules **17**(4), 4484–4497 (2012).

[92]M. Grätzel, "Photoelectrochemical cells," in *Materials for Sustainable Energy: A Collection of Peer-Reviewed Research and Review Articles* (Nature Publishing Group, 2011), pp. 26–32.

[93]M. R. Wasielewski, "Self-assembly strategies for integrating light harvesting and charge separation in artificial photosynthetic systems," Acc. Chem. Res. **42**(12), 1910–1921 (2009).

[94]F. D'Souza and O. Ito, "Supramolecular donor–acceptor hybrids of porphyrins/phthalocyanines with fullerenes/carbon nanotubes: Electron transfer, sensing, switching, and catalytic applications," Chem. Commun. **2009**(33), 4913–4928.

[95]D. Gust, T. A. Moore, and A. L. Moore, "Solar fuels via artificial photosynthesis," Acc. Chem. Res. **42**(12), 1890–1898 (2009).

[96]H. Imahori and S. Fukuzumi, "Porphyrin-and fullerene-based molecular photovoltaic devices," Adv. Funct. Mater. **14**(6), 525–536 (2004).

[97]A. K. Burrell, D. L. Officer, P. G. Plieger, and D. C. Reid, "Synthetic routes to multiporphyrin arrays," Chem. Rev. **101**(9), 2751–2796 (2001).

[98]T. D. Santos, A. Morandeira, S. Koops, A. J. Mozer, G. Tsekouras, Y. Dong, P. Wagner, G. Wallace, J. C. Earles, K. C. Gordon, and D. Officer, "Injection limitations in a series of porphyrin dye-sensitized solar cells," J. Phys. Chem. C **114**(7), 3276–3279 (2010).

[99]T. Bessho, S. M. Zakeeruddin, C. Y. Yeh, E. W. G. Diau, and M. Grätzel, "Highly efficient mesoscopic dye-sensitized solar cells based on donor–acceptor-substituted porphyrins," Angew. Chem. Int. Ed. **49**(37), 6646–6649 (2010).

[100]A. Baba, K. Wakatsuki, K. Shinbo, K. Kato, and F. Kaneko, "Increased short-circuit current in grating-coupled surface plasmon resonance field-enhanced dye-sensitized solar cells," J. Mater. Chem. **21**(41), 16436–16441 (2011).

[101]K. Magsi, P. Lee, Y. Kang, S. Bhattacharya, and, C. M. Fortmann, "Enhanced chlorophyll a purification and dye sensitized solar cell performance," MRS Online Proc. Lib. Arch. **1390**, mrsf11-1390-h13-36 (2012).

[102]C. S. Chou, R. Y. Yang, M. H. Weng, and C. H. Yeh, "Preparation of TiO$_2$/dye composite particles and their applications in dye-sensitized solar cell," Powder Technol. **187**(2), 181–189 (2008).

[103]W. Mekprasart, W. Jarernboon, and W. Pecharapa, "TiO$_2$/CuPc hybrid nanocomposites prepared by low-energy ball milling for dye-sensitized solar cell application," Mater. Sci. Eng. B **172**(3), 231–236 (2010).

[104]S. D. Delekar, A. G. Dhodamani, K. V. More, T. D. Dongale, R. K. Kamat, S. F. Acquah, N. S. Dalal, and D. K. Panda, "Structural and optical properties of nanocrystalline TiO$_2$ with multiwalled carbon nanotubes and its photovoltaic studies using Ru (II) sensitizers," ACS Omega **3**(3), 2743–2756 (2018).

[105]H. Deng, Y. Zhou, H. Mao, and Z. Lu, "The mixed effect of phthalocyanine and porphyrin on the photoelectric conversion of a nanostructured TiO$_2$ electrode," Synth. Met. **92**(3), 269–274 (1998).

[106]P. Balraju, M. Kumar, M. S. Roy, and G. D. Sharma, "Dye sensitized solar cells (DSSCs) based on modified iron phthalocyanine nanostructured TiO$_2$ electrode and PEDOT:PSS counter electrode," Synth. Met. **159**(13), 1325–1331 (2009).

[107]E. Palomares, M. V. Martínez-Díaz, S. A. Haque, T. Torres, and J. R. Durrant, "State selective electron injection in non-aggregated titanium phthalocyanine sensitised nanocrystalline TiO$_2$ films," Chem. Commun. **2004**(18), 2112–2113.

[108]R. B. Koehorst, G. K. Boschloo, T. J. Savenije, A. Goossens, and T. J. Schaafsma, "Spectral sensitization of TiO2 substrates by monolayers of porphyrin heterodimers," J. Phys. Chem. B **104**(10), 2371–2377 (2000).

[109]Y. Amao and T. Komori, "Bio-photovoltaic conversion device using chlorine-e6 derived from chlorophyll from spirulina adsorbed on a nanocrystalline TiO2 film electrode," Biosens. Bioelectron. **19**(8), 843–847 (2004).

[110]S. A. Taya, T. M. El-Agez, K. S. Elrefi, and M. S. Abdel-Latif, "Dye-sensitized solar cells based on dyes extracted from dried plant leaves," Turk. J. Phys. **39**(1), 24–30 (2015).

[111]H. C. Hassan, Z. H. Z. Abidin, F. I. Chowdhury, and A. K. Arof, "A high efficiency chlorophyll sensitized solar cell with quasi solid PVA based electrolyte," Int. J. Photoenergy **2016**, 3685210.

[112]M. Alhamed, A. S. Issa, and A. W. Doubal, "Studying of natural dyes properties as photo-sensitizer for dye sensitized solar cells (DSSC)," J. Electron Devices **16**(11), 1370–1383 (2012).

[113]I. Kartini, L. Dwitasari, T. D. Wahyuningsih, C. Chotimah, and L. Wang, "Sensitization of xanthophylls-chlorophyllin mixtures on titania solar cells," Int. J. Sci. Eng. **8**(2), 109–114 (2015).

[114]D. D. Pratiwi, F. Nurosyid, Kusumandari, A. Supriyanto, and R. Suryana, "Effect of Ni doping into chlorophyll dye on the efficiency of dye-sensitized solar cells (DSSC)," AIP Conf. Proc. **2014**(1), 020066 (2018).

[115]C. W. Lee, H. P. Lu, C. M. Lan, Y. L. Huang, Y. R. Liang, W. N. Yen, Y. C. Liu, Y. S. Lin, E. W. G. Diau, and C. Y. Yeh, "Novel zinc porphyrin sensitizers for dye-sensitized solar cells: Synthesis and spectral, electrochemical, and photovoltaic properties," Chem. Eur. J. **15**(6), 1403–1412 (2009).

[116]S. L. Wu, H. P. Lu, H. T. Yu, S. H. Chuang, C. L. Chiu, C. W. Lee, E. W. G. Diau, and C. Y. Yeh, "Design and characterization of porphyrin sensitizers with a push-pull framework for highly efficient dye-sensitized solar cells," Energy Environ. Sci. **3**(7), 949–955 (2010).

[117]A. J. Mozer, M. J. Griffith, G. Tsekouras, P. Wagner, G. G. Wallace, S. Mori, K. Sunahara, M. Miyashita, J. C. Earles, K. C. Gordon, and L. Du, "Zn−Zn porphyrin dimer-sensitized solar cells: Toward 3-D light harvesting," J. Am. Chem. Soc. **131**(43), 15621–15623 (2009).

[118]H. Otaka, M. Kira, K. Yano, S. Ito, H. Mitekura, T. Kawata, and F. Matsui, "Multi-colored dye-sensitized solar cells," J. Photochem. Photobiol. A: Chem. **164**(1–3), 67–73 (2004).

[119]R. Y. Ogura, S. Nakane, M. Morooka, M. Orihashi, Y. Suzuki, and K. Noda, "High-performance dye-sensitized solar cell with a multiple dye system," Appl. Phys. Lett. **94**(7), 073308 (2009).

[120]S. R. Wenham, *Applied Photovoltaics* (Routledge, 2011).

[121]A. A. Husain, W. Z. W. Hasan, S. Shafie, M. N. Hamidon, and S. S. Pandey, "A review of transparent solar photovoltaic technologies," Renewable Sustainable Energy Rev. **94**, 779–791 (2018).

[122]Y. Li, X. Guo, Z. Peng, B. Qu, H. Yan, H. Ade, M. Zhang, and S. R. Forrest, "Color-neutral, semitransparent organic photovoltaics for power window applications," Proc. Nat. Acad. Sci. U.S.A **117**(35), 21147–21154 (2020).

[123]A. Colsmann, A. Puetz, A. Bauer, J. Hanisch, E. Ahlswede, and U. Lemmer, "Efficient semi-transparent organic solar cells with good transparency color perception and rendering properties," Adv. Energy Mater. **1**(4), 599–603 (2011).

[124]C. L. Cheng, C. S. S. Jimenez, and M. C. Lee, "Research of BIPV optimal tilted angle, use of latitude concept for south orientated plans," Renewable Energy **34**(6), 1644–1650 (2009).

[125]Y. Chen, A. K. Athienitis, and K. Galal, "Modeling, design and thermal performance of a BIPV/T system thermally coupled with a ventilated concrete slab in a low energy solar house: Part 1, BIPV/T system and house energy concept," Sol. Energy **84**(11), 1892–1907 (2010).

[126]B. Liu, S. Duan, and T. Cai, "Photovoltaic DC-building-module-based BIPV system—Concept and design considerations," IEEE Trans. Power Electron. **26**(5), 1418–1429 (2011).

[127]J. H. Yoon, S. R. Shim, Y. S. An, and K. H. Lee, "An experimental study on the annual surface temperature characteristics of amorphous silicon BIPV window," Energy Build. **62**, 166–175 (2013).

[128]H. Alrashidi, A. Ghosh, W. Issa, N. Sellami, T. K. Mallick, and S. Sundaram, "Thermal performance of semitransparent CdTe BIPV window at temperate climate," Sol. Energy **195**, 536–543 (2020).

[129]O. Ellabban, H. Abu-Rub, and F. Blaabjerg, "Renewable energy resources: Current status, future prospects and their enabling technology," Renewable Sustainable Energy Rev. **39**, 748–764 (2014).

[130]M. S. Dresselhaus and I. L. Thomas, "Alternative energy technologies," Nature **414**(6861), 332–337 (2001).

[131]M. Grätzel, "Solar energy conversion by dye-sensitized photovoltaic cells," Inorg. Chem. **44**(20), 6841–6851 (2005).

[132]R. H. Bube, *Photovoltaic Materials* (Imperial College Press, London, 1998).

[133]P. Irace, and H. Brandon, "Solar heating in commercial buildings," in *Mechanical Engineering and Materials Science Independent Study.* 50 (Washington University, St. Louis, 2017), see https://openscholarship.wustl.edu/mems500/50.

[134]See https://greenecon.net/understanding-the-cost-of-solar-energy/energy_economics.html for "Understanding the Cost of Solar Energy—Green Econometrics" (last accessed October 28, 2020).

[135]I. Nath, "Cleaning up after clean energy: Hazardous waste in the solar industry," Stanford J. Int. Relat. **11**(2), 6–15 (2010).

[136]K. W. Kizer, L. G. Garb, and C. H. Hine, "Health effects of silicon tetrachloride. Report of an urban accident," J. Occup. Med.: Off. Publ. Ind. Med. Assoc. **26**(1), 33–36 (1984).

[137]See https://news.energysage.com/solar-panels-toxic-environment/ for "Are Solar Panels Toxic to the Environment?" (last accessed October 28, 2020).